Design, synthesis, and biological evaluation of novel dipeptide-type SARS-CoV 3CL protease inhibitors: Structure-activity relationship study

ARTICLE *in* EUROPEAN JOURNAL OF MEDICINAL CHEMISTRY · MAY 2013

Impact Factor: 3.45 · DOI: 10.1016/j.ejmech.2013.05.005 · Source: PubMed

European Journal of Medicinal Chemistry 65 (2013) 436–447

Contents lists available at SciVerse ScienceDirect

European Journal of Medicinal Chemistry

journal homepage: http://www.elsevier.com/locate/ejmech

Original article

Design, synthesis, and biological evaluation of novel dipeptide-type SARS-CoV 3CL protease inhibitors: Structure–activity relationship study

Pillaiyar Thanigaimalai [a], Sho Konno [a], Takehito Yamamoto [a], Yuji Koiwai [a], Akihiro Taguchi [a], Kentaro Takayama [a], Fumika Yakushiji [a], Kenichi Akaji [b], Yoshiaki Kiso [b], Yuko Kawasaki [c], Shen-En Chen [c], Aurash Naser-Tavakolian [c], Arne Schön [c], Ernesto Freire [c], Yoshio Hayashi [a,*]

[a] Department of Medicinal Chemistry, Tokyo University of Pharmacy and Life Sciences, Tokyo 192-0392, Japan
[b] Department of Medicinal Chemistry, Kyoto Pharmaceutical University, Kyoto 607-8412, Japan
[c] Department of Biology, Johns Hopkins University, Baltimore, MD, USA

ARTICLE INFO

Article history:
Received 11 March 2013
Received in revised form
20 April 2013
Accepted 7 May 2013
Available online 20 May 2013

Keywords:
SARS
SARS-CoV 3CL protease
Peptidomimetics
Dipeptide
Cysteine protease inhibitors
Docking study

ABSTRACT

This work describes the design, synthesis, and evaluation of low-molecular weight peptidic SARS-CoV 3CL protease inhibitors. The inhibitors were designed based on the potent tripeptidic Z-Val-Leu-Ala(-pyrrolidone-3-yl)-2-benzothiazole (**8**; K_i = 4.1 nM), in which the P3 valine unit was substituted with a variety of distinct moieties. The resulting series of dipeptide-type inhibitors displayed moderate to good inhibitory activities against $3CL^{pro}$. In particular, compounds **26m** and **26n** exhibited good inhibitory activities with K_i values of 0.39 and 0.33 μM, respectively. These low-molecular weight compounds are attractive leads for the further development of potent peptidomimetic inhibitors with pharmaceutical profiles. Docking studies were performed to model the binding interaction of the compound **26m** with the SARS-CoV 3CL protease. The preliminary SAR study of the peptidomimetic compounds with potent inhibitory activities revealed several structural features that boosted the inhibitory activity: (i) a benzothiazole warhead at the S1′ position, (ii) a γ-lactam unit at the S1-position, (iii) an appropriately hydrophobic leucine moiety at the S2-position, and (iv) a hydrogen bond between the *N*-arylglycine unit and a backbone hydrogen bond donor at the S3-position.

1. Introduction

Since its first appearance in Southern China in late 2002, severe acute respiratory syndrome (SARS) has been recognized as a global threat [1,2]. Its rapid and unexpected spread to 32 countries has affected more than 8000 individuals and caused nearly 800 (~10%) fatalities worldwide within a few months [1–3]. The causative SARS pathogen is a novel coronavirus, SARS-CoV [4,5]. SARS-CoV is a positive-strand RNA virus with a genome sequence that is only moderately homologous to other known coronaviruses [6,7]. SARS-CoV encodes a chymotrypsin-like protease ($3CL^{pro}$), also referred to as the main protease (M^{pro}), which plays a pivotal role in processing viral polyproteins and controlling replicase complex activity [8]. This enzyme is indispensable for viral replication and infection processes, making it an ideal target for the design of antiviral therapies. The $3CL^{pro}$ active site contains a catalytic dyad in which a cysteine residue (Cys145) acts as a nucleophile and a histidine (His41) residue acts as a general acid or base [9,10]. The SARS epidemic was successfully controlled in 2003; however, the potential reemergence of pandemic SARS-CoV continues to pose a risk, and new strains of SARS could potentially be more virulent than the strains that contributed to the 2003 outbreak. Since 2003, two additional human coronaviruses, NL63 and HKU1, have been identified in patients around the world [11,12]. Recently, a new SARS-like virus, HCoV-EMC, was identified in at least two individuals, one of whom died [13]. Very recently, the first case of a fatal respiratory illness similar to the deadly SARS was confirmed in Britain [14]. The World Health Organization (WHO) has announced that it is closely monitoring the situation and is working to “ensure a high degree of preparedness,

* Corresponding author. Tel./fax: +81 42 676 3275.
E-mail address: yhayashi@toyaku.ac.jp (Y. Hayashi).

0223-5234/$ – see front matter © 2013 Elsevier Masson SAS. All rights reserved.
http://dx.doi.org/10.1016/j.ejmech.2013.05.005

should the new virus be found to be sufficiently transmissible to cause a community outbreak". There is a significant need to develop anti-SARS agents that are capable of treating this potentially fatal respiratory illness. Several reports of crystalline forms of the SARS-CoV 3CL^{pro} protein bound to hexapeptidyl chloromethyl ketone inhibitors have been reported [6,9], and numerous peptidic structures have been reported in the context of targeted antiviral drug design [15–22]. The reported protease inhibitors are generally peptidic in nature, often five to three residues in length, and bear a reactive warhead group at the *C*-terminus which forms an interaction with the protease catalytic Cys145 (Fig. 1, **1**–**9**). Two of these compounds (**8** and **9**), recently described in a separate report from our group [22], exhibited excellent potent inhibitory activities with K_i values of 4.1 and 3.1 nM, respectively. These peptidic inhibitors provided valuable insight into the design constraints for this system and quickly led to the development of non-peptidic small molecule inhibitors (Fig. 1, **10**–**17**) [23–30]. These small molecular inhibitors generally showed moderate to good activities.

Recently, we performed a structure–activity relationship study based on the lead compound, Z-Val-Leu-Ala(pyrrolidone-3-yl)-2-thiazole (**7**) [21]. This study led to the discovery of the potent compounds **8** and **9**, with K_i values in the low nanomolar range [22].

Extending our studies toward the development of new anti-SARS agents, we now report the design, synthesis, and evaluation of a series of low-molecular weight dipeptide-type compounds in which the P3 valine unit is removed from the previous lead Z-Val-Leu-Ala(pyrrolidone-3-yl)-2-benzothiazole compound (**8**, Fig. 1). A preliminary SAR study led to the identification of inhibitors with moderate to good inhibitory activities. In particular, compounds **26m** and **26n** exhibited potent inhibitory activities with K_i values of 0.39 and 0.33 μM, respectively. The binding interactions of **26m** were predicted using molecular modeling studies. We describe the results of these extensive studies in detail, including the design, synthesis, molecular modeling, and biological evaluation of a series of SARS-CoV 3CL^{pro} inhibitors.

2. Results and discussion

2.1. Synthesis

The synthesis of the title inhibitors was achieved through a coupling reaction involving two key fragments, as shown in Scheme 1. One of the key fragment intermediates (**19**) was synthesized from the amino acid esters **18** with either corresponding carboxylic acids *via* 1-ethyl-3-(3-dimethylaminopropyl)carbodiimide hydrochloride–1-hydroxybenzotriazole (EDC·HCl–HOBt)

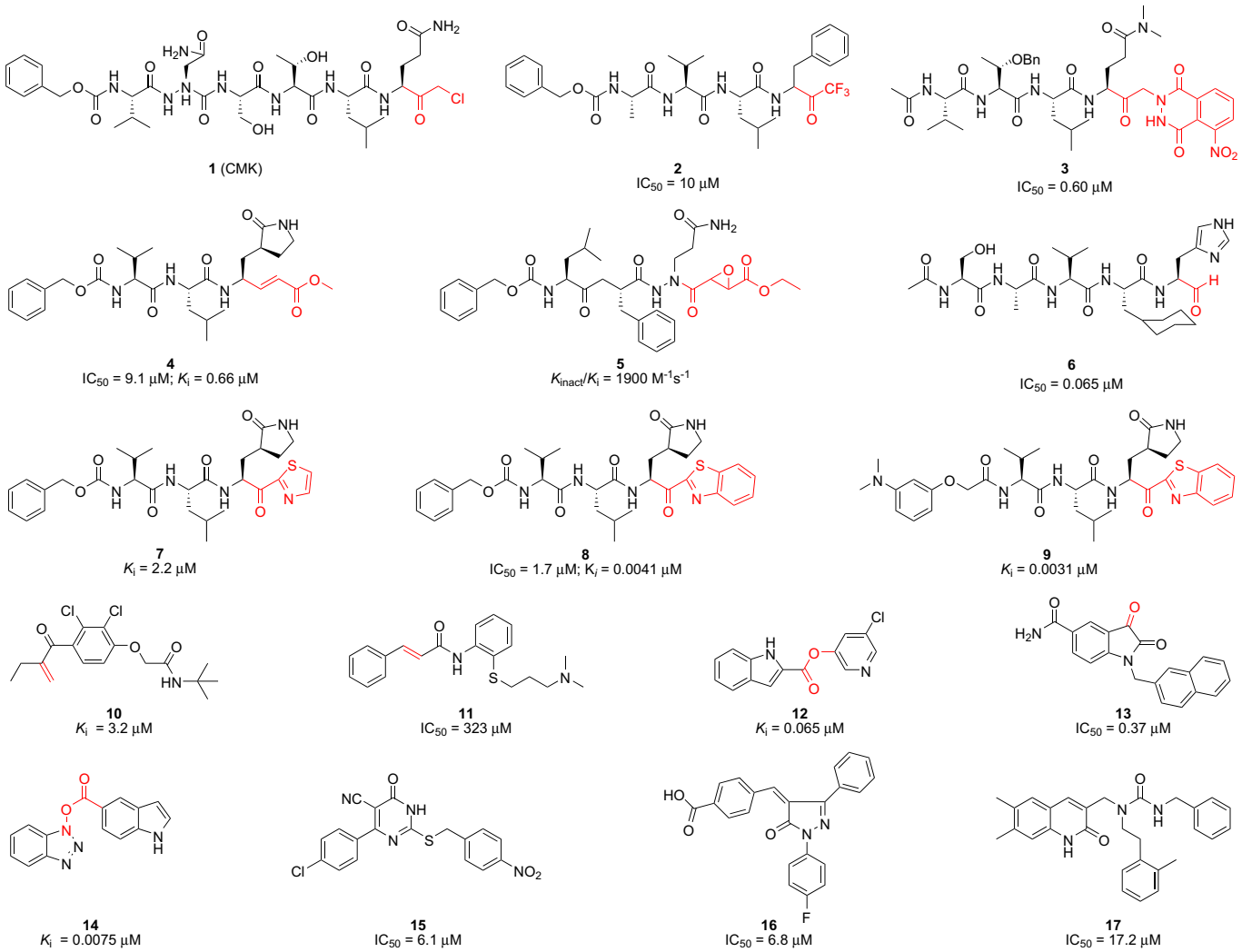

Fig. 1. Representative peptidomimetics (**1**–**9**) and small molecular (**10**–**17**) 3CL^{pro} inhibitors highlighting reactive warhead groups (red).

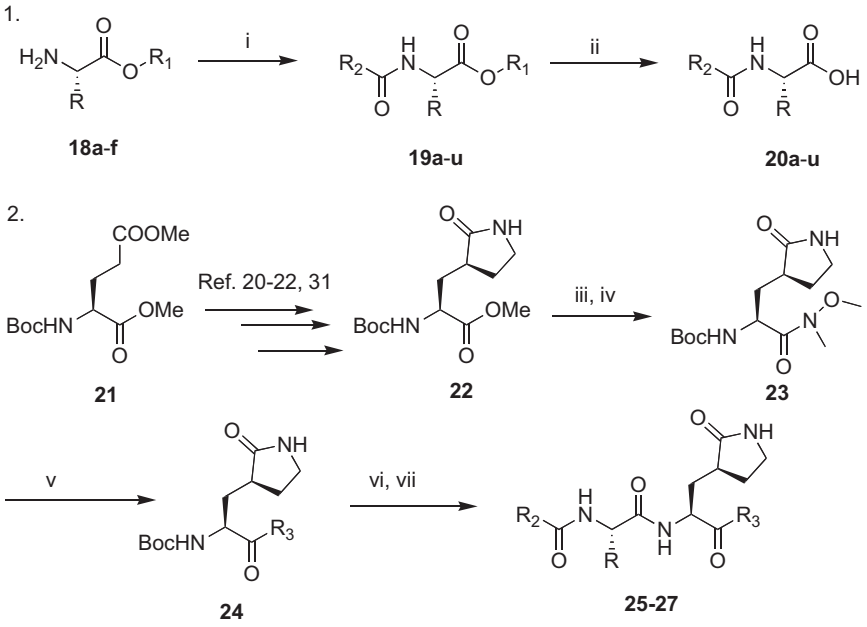

Scheme 1. Reagents and conditions: i) EDC·HCl, HOBt·H_2O, TEA/DMF (if reactant is a carboxylic acid) or Et_3N/CH_2Cl_2 (if reactant is a benzyloxycarbonyl chloride), 0 °C–rt; ii) TFA/H_2O, CH_2Cl_2 (if R_1 = *tert*-butyl unit), or LiOH·H_2O, THF/H_2O, (if R_1 = methyl unit); iii) 4M NaOH, MeOH; iv) HN(OMe)Me·HCl, EDC·HCl, HOBt·H_2O, Et_3N/DMF, 0 °C–rt; v) *n*-BuLi, THF, −78 °C (if R_3 = benzothiazole) or LDA, THF, −78 °C (if R_3 = 5-arylated thiazoles); vi) TFA/H_2O (10:1), CH_2Cl_2; vii) **20**, HBTU, DIPEA/DMF, 0 °C–rt followed by HPLC purification. Note: The substituents R–R_3 are indicated in Tables 1–3

mediated coupling in the presence of triethylamine (TEA) in DMF or acid chlorides in the presence of TEA in dichloromethane (CH_2Cl_2). The resulting *N*-protected amino acid esters (**19**) were consequently deprotected in the presence of TFA or lithium hydroxide·water (LiOH·H_2O) to afford the *N*-protected amino acids (**20**), which were used directly in the subsequent step.

The γ-lactam-thiazoles (**24**) were synthesized using an approach similar to the syntheses reported previously [21,22,31]. Accordingly, the optically pure L-glutamic acid ester **21** was converted to the γ-lactam ester **22** by treatment with bromoacetonitrile, followed by reduction with PtO_2 (5%) and cyclization. The resulting ester **22** was hydrolyzed in the presence of 4 M NaOH in methanol to yield the corresponding acid, which was coupled to *N*,*O*-dimethylhydroxylamine *via* the EDC–HOBt method to afford the Weinreb amide **23**. The Weinreb amide **23** was then coupled to the appropriate thiazoles in the presence of *n*-butyl lithium (*n*-BuLi) or lithium diisopropylamide (LDA) at −78 °C to afford the γ-lactam-thiazoles **24**. The Boc protecting group was then removed, and the resulting intermediate was subsequently reacted with the above-mentioned *N*-protected amino acids **20** in the presence of *O*-benzotriazole-*N*,*N*,*N*′,*N*′-tetramethyluroniumhexafluoro phosphate (HBTU) and DIPEA in DMF to afford the title compounds **25**–**27**. All compounds were purified by reverse phase HPLC and characterized by ^1H and ^{13}C NMR, and mass spectrometry analysis. The purity of each compound exceeded 90–95%.

2.2. Biological activity

The compounds were subjected to a fluorometric protease inhibitory assay against SARS-CoV $3CL^{pro}$, as described previously [32,33]. Briefly, the kinetic parameters were determined at a constant substrate concentration, and the inhibitor concentrations were varied to assess the K_i values [22]. The IC_{50} values were determined only for certain potent inhibitors, based on the apparent decrease in the substrate concentration (H-Thr-Ser-Ala-Val-Leu-Gln-Ser-Gly-Phe-Arg-Lys-NH_2) upon digestion by R188I SARS $3CL^{pro}$, as described previously [19,34]. The cleavage reaction was monitored by analytical HPLC, and the cleavage rates were calculated from the decrease in the substrate peak area. Tables 1–4 report the K_i or IC_{50} values as the mean of 3 independent experiments.

In an effort to develop low-molecular weight peptidic SARS-CoV $3CL^{pro}$ inhibitors, we designed a series of dipeptide-type inhibitors based on the previous potent lead compound **8** (see Fig. 1). In a first attempt, the P3 valine region was removed and the P4-benzyloxycarbonyl (Cbz) in **8** was replaced with a series of small moieties with sizes similar to that of the P3 valine group in **8**. The inhibitory activities of the resulting dipeptidic compounds bearing a valine mimic, isopentanoyl (**25a**; K_i = 5.9 μM) or *tert*-butoxy carbonyl (**25b**; K_i = 23 μM), were dramatically reduced compared to the activity of **8** (K_i = 0.0041 μM) [22]; however, the introduction of Cbz (**25c**; K_i and IC_{50} = 0.46 and 21.0 μM) as a P3 moiety resulted in a 12-fold or 50-fold activity increase for **25a** or **25b**, respectively, although the potency was reduced relative to the value for the tripeptidic lead **8**. This result suggested that the Cbz group, which was introduced in place of the P3 scaffold in the dipeptidic **25c**, conveyed appreciable activity; therefore, compound **25c** could serve as a lead for further optimization steps. By retaining the P3 Cbz moiety in **25c**, we examined the relevance of the leucine residue (or isobutyl unit) for P2 substrate selectivity in comparison with a variety of its congeners. Accordingly, a series of isosteres was introduced, including *n*-butyl (**25d**; K_i = 1.60 μM), isopropyl (**25e**; K_i = 1.71 μM), *sec*-butyl (**25f**; K_i = 29.0 μM), 3-methyl(thio)ethyl (**25g**; K_i = 9.40 μM), and benzyl (**25h**; K_i = 1.20 μM). The compounds bearing *n*-butyl (**25d**), isopropyl (**25e**), or benzyl (**25h**) groups exhibited reasonable inhibitory activities, although the potencies were reduced by a factor of 3–4 relative to the value for **25c**. The inhibitory activity of the compound bearing *sec*-butyl (**25f**) or 3-methyl(thio)ethyl (**25g**) was severely reduced compared to the activity of **25c**. Therefore, the leucine residue (or isobutyl group) was more selective and appropriate as a P2 group in **25c**, providing enhanced inhibitory activity.

The P3 moiety of the lead compound **25c** was examined by introducing a wide variety of substituents, such as aryl (or

Table 1
SARS-CoV 3CL^{pro} inhibitory activities (K_i) of **25a**–**h**.

Entry no.	Inhibitors	K_i (μM)	Entry no.	Inhibitors	K_i (μM)
25a	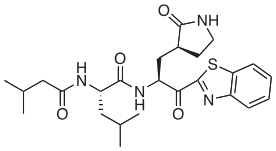	5.90	**25e**	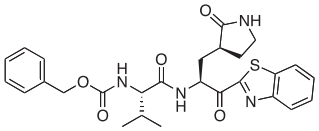	1.71
25b	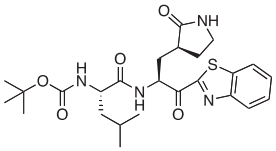	23.0	**25f**	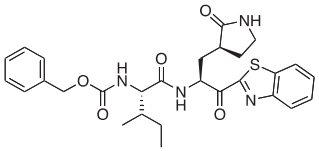	29.0
25c	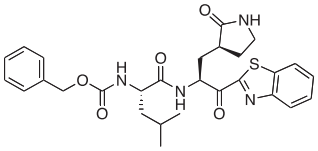	0.46	**25g**	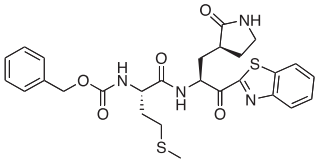	9.40
25d	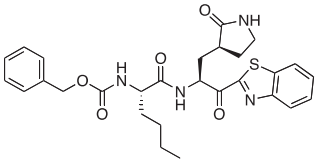	1.60	**25h**	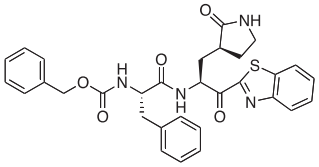	1.20

heteroaryl) acetyls and propionyls, arylacrylyls, aryloxyacetyls, and *N*-arylglycyls. Initially, the aryl (or heteroaryl) acetyls and propionyls were introduced, including phenylacetyl (**26a**; $K_i = 3.20$ μM), 4-methoxyphenylacetyl (**26b**; K_i and $IC_{50} = 0.42$ and 43 μM), 4-methoxyphenylpropionyl (**26c**; $K_i = 0.62$ μM), and pyridine-3-propionyl (**26d**; $K_i = 7.4$ μM). Among the compounds, a 4-methoxyphenylacetyl derivative (**26b**) exhibited potent inhibitory activity; the phenylacetyl (**26a**) and pyridine-3-propionyl (**26d**) derivatives in particular displayed low inhibitory activities. Therefore, the 4-methoxyphenylacetyl moiety provided a good alternative to the P3 Cbz group in **25c**. We next introduced the arylacrylyls, including cinnamoyl (**26e**; $K_i = 0.69$ μM), 4-methoxycinnamoyl (**26f**; $K_i = 0.70$ μM), and 3,4-dimethoxycinnamoyl (**26g**; $K_i = 1.30$ μM). These compounds showed moderate inhibitory activities relative to the lead **25c**; thus, the acrylyls were not considered further as P3 moieties in the context of **25c**.

A previous report describing a SAR study of the tripeptidomimetic **7** (see Fig. 1) as a SARS inhibitor revealed that the introduction of an aryloxyacetyl at the *N*-terminal position (the P4 position) appeared to significantly enhance the inhibitory activity against SARS-CoV 3CL^{pro} [22]. Therefore, we introduced a series of aryloxyacetyls, including phenoxyacetyl (**26h**; K_i and $IC_{50} = 0.56$ and 24 μM), 4-methoxyphenoxyacetyl (**26i**; $K_i = 1.56$ μM), 4-hydroxyphenoxyacetyl (**26j**; $K_i = 8.4$ μM), and 3-dimethyl aminophenoxyacetyl (**26k**; $K_i = 0.84$ μM) as P3 groups in place of the Cbz group in **25c**. Compounds **26h** and **26k** exhibited comparable activities to **25c**; however, the other derivatives (**26i** and **26j**) displayed reduced inhibitory activities relative to the lead compound **25c**. These results suggested that the introduction of an aryloxyacetyl P3 group in the dipeptidic **25c** did not appreciably improve the inhibitory activity against 3CL^{pro}. We also introduced several *N*-arylglycyls, including *N*-(4-methoxyphenyl)glycyl (**26l**; $K_i = 3.20$ μM), *N*-(3-methoxyphenyl)glycyl (**26m**; K_i and $IC_{50} = 0.39$ and 10.0 μM), and *N*-(2-methoxyphenyl)glycyl (**26n**; K_i and $IC_{50} = 0.33$ and 14.0 μM). The results of these studies revealed that compounds **26m** and **26n** displayed relatively potent inhibitory activities compared to the lead **25c**. The compound bearing an *N*-(2-methoxyphenyl)glycyl (**26n**) was identified as the most potent inhibitor in the present study. This result suggested that the hydrogen bonding properties of the amino group on the *N*-arylglycyl moiety might have contributed to the improvement in activity (see Fig. 2B).

The P1′ moiety was examined next by varying the 5-substituted thiazoles (**27a**–**d**). The inhibitory activities of compounds **27a**–**d** are illustrated in Table 3. Inhibitor **27a** exhibited an inhibitory activity comparable to that of **25c**. The other 5-arlylated thiazoles (**27b**–**d**) generally exhibited very low inhibitory activities compared to **25c**. These studies confirmed that the benzothiazole unit was more suitable as a warhead group on the P1′ moiety in **25c**.

2.3. Molecular docking study

The binding mode of compound **26m** with 3CL^{pro} was simulated using a molecular docking program as described previously [22]. We examined the molecular docking of the potent active compound **26m** in comparison with docking of the tripeptidic **9** and a structurally similar ligand, the docking structure of which has been elucidated previously by X-ray crystallography (PDB ID: 1WOF, $K_i = 10.7$ μM) (Fig. 2) [35]. Several minimization processes were performed using the MMFF94X force field to model the solvation environment surrounding the inhibitor. A molecular simulation was then performed. As shown in Fig. 2A, the P1′–P2 moieties in **26m**, in the tripeptidic compound **9**, and in the original ligand interacted with the same region of the protease. Interestingly, the aminoacetyl group on the *N*-(3-methoxyphenyl)glycyl group in **26m** mimicked the P3 valine moieties of the tripeptidomimetic **9** and the reported ligand. The interactions of compound **26m** with the protein are described in detail in Fig. 2B. Particularly, a notable hydrogen bonding involved between the amino group (–NH) of P3 *N*-(3-methoxyphenyl)glycine with a backbone amino acid residue Glu166 of 3CL^{pro} was observed to have relatively potent inhibition than other inhibitors presented in the study against SARS-CoV

Table 2
SARS-CoV 3CL^{pro} inhibitory activities (K_i) of **26a**–**n**.

Entry No.	Inhibitors	K_i (μM)	Entry No.	Inhibitors	K_i (μM)
26a	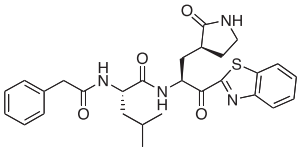	3.20	**26h**	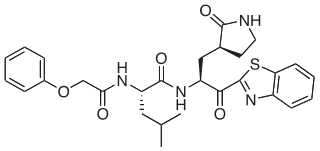	0.56
26b	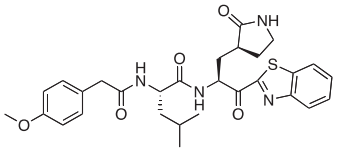	0.42	**26i**	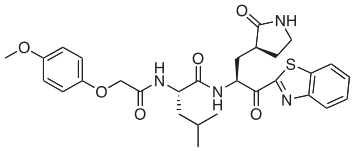	1.56
26c	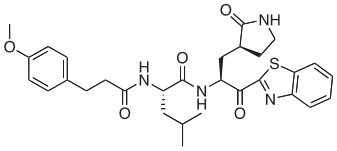	0.61	**26j**	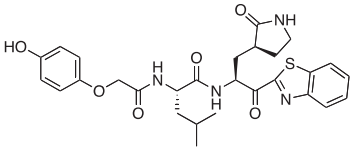	8.4
26d	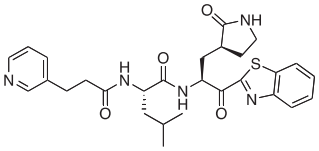	7.4	**26k**	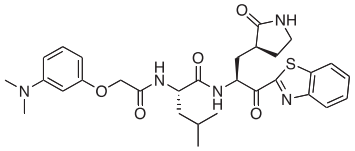	0.84
26e	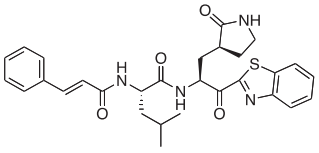	0.69	**26l**	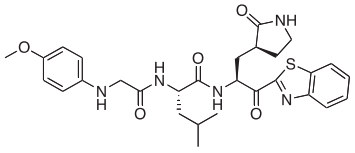	3.20
26f	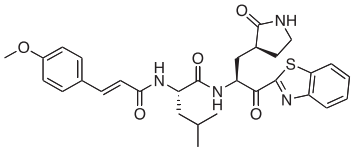	0.70	**26m**	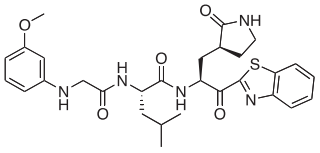	0.39
26g	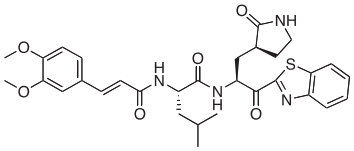	1.30	**26n**	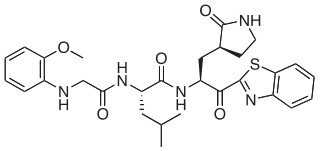	0.33

3CL^{pro}. The essential nature of this hydrogen bond will be explored in further optimization studies of dipeptide-type SARS-CoV 3CL^{pro} inhibitors.

3. Conclusion

In an effort to develop low-molecular weight peptidic anti-SARS agents, we designed, synthesized, and evaluated a series of dipeptide-type inhibitors in which the P3 valine unit in our potent tripeptidomimetic lead compound **8** was replaced with a number of distinct functionalities. In a preliminary study, the compound **25c**, bearing a benzyloxycarbonyl (Cbz) P3 moiety, was identified as a lead compound. The P3 moiety in **25c** was systematically modified with a view to improve the biological activity. This study led to the identification of a compound bearing an *N*-arylglycyl as a P3 moiety as having higher inhibitory activity due to the presence of a hydrogen bond with the backbone amino acid residue Glu166 of 3CL^{pro}. Leucine and benzothiazole units were identified as appropriate P2 and P1′ moieties, respectively, in **25c**. Accordingly, compounds **26m** and **26n** were recognized as potent inhibitors in the present study. These potent dipeptidic inhibitors provide attractive leads, which are undergoing further structural modifications in an effort to improve the pharmaceutical profiles. These processes are underway and will be reported in the near future.

4. Experimental section

4.1. Materials and methods

Reagents and solvents were purchased from Wako Pure Chemical Ind., Ltd. (Osaka, Japan), and Aldrich Chemical Co. Inc. (Milwaukee, WI) and were used without further purification. Analytical thin-layer chromatography (TLC) was performed on Merck Silica Gel 60F254 pre-coated plates. Preparative HPLC was performed using a C18 reverse-phase column (19 × 150 mm; Sun-Fire Prep C18

Table 3
SARS-CoV 3CL^{pro} inhibitory activities (K_i) of **27a**–**d**.

Entry no.	Inhibitors	K_i (μM)
27a	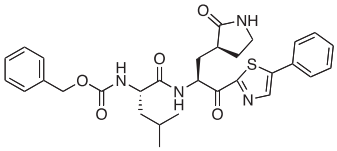	0.66
27b	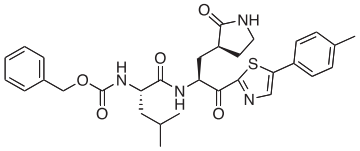	37.0
27c	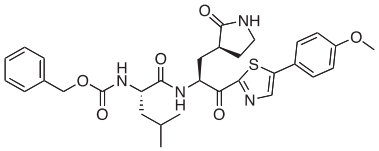	52.0
27d	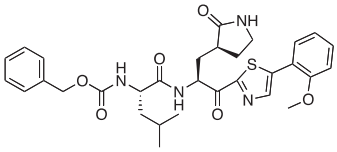	2.50

OBD™, 5 μm) with a binary solvent system: a linear gradient of CH_3CN in 0.1% aqueous TFA at a flow rate of 6 mL/min, detected at UV 254 and 230 nm. All solvents used for HPLC were HPLC-grade. All other chemicals were of analytical grade or better. ^1H and ^{13}C NMR spectra were obtained using a JEOL 400 MHz spectrometer, a Varian Mercury 300 spectrometer (300 MHz), or a BRUKER AV600 spectrometer (600 MHz) with tetramethylsilane as an internal standard. High-resolution mass spectra (ESI or EI) were recorded on a micromass Q-Tof Ultima API or a JEOL JMS-GCmate BU-20 spectrometer. Mass spectra (ESI) were recorded on an LCMS-2010EV (SHIMADZU).

4.2. Synthetic procedures

4.2.1. Synthetic procedures for the preparation of (S)-tert-butyl 2-(3-methylbutanamido)-4-methylpentanoate (**19a**)

To a solution of the commercially available L-leucine *tert*-butyl ester **18a** (0.200 g, 0.89 mmol) in DMF (15 mL) was added an isovaleric acid (0.100 g, 0.98 mmol), HOBt·H_2O (0.151 g, 0.98 mmol), and EDC·HCl (0.189 g, 0.98 mmol). The resulting solution was cooled to 0 °C under ice bath conditions, and TEA was then added dropwise. After 5 min, the ice bath was removed and the mixture was allowed to stir for 2 h at ambient temperature. DMF was removed under high vacuum, and the resulting residue was dissolved in EtOAc (30 mL). The organic layer was washed with 5% citric acid (20 mL × 2), 5% $NaHCO_3$ (20 mL × 2), and brine (20 mL). The solution was dried over Na_2SO_4, filtered, and evaporated under reduced pressure to give compound **19a**. The resulting crude compound was purified by silica gel column chromatography using hexane–EtOAc as eluents. Yield 65%; white solid; ^1H NMR (400 MHz, CD_3OD): δ 4.20 (t, J = 7.6 Hz, 1H), 2.03–1.90 (m, 3H), 1.57–1.42 (m, 3H), 1.34 (s, 9H), 0.86–0.79 (m, 12H). HRMS (ESI): m/z calcd for $C_{15}H_{30}NO_3$ $[M + H]^+$ 272.2226, found 272.2230.

The intermediates **19h**–**u** were prepared from L-leucine *tert*-butyl ester **18a** and various commercially available carboxylic acids according to the procedure described for the synthesis of **19a**.

4.2.2. Synthesis of benzyl (S)-1-(tert-butoxycarbonyl)-3-methyl butylcarbamate (**19b**)

To a solution of the commercially available L-leucine *tert*-butyl ester **18a** (0.500 g, 2.20 mmol) in CH_2Cl_2 (20 mL) was added benzyloxycarbonyl chloride (0.410 mL, 2.5 mmol). The resulting solution was cooled to 0 °C and TEA (0.380 mL, 2.5 mmol) was then added dropwise. After 5 min, the ice bath was removed and the mixture was allowed to stir for 2 h at room temperature. The mixture was washed with H_2O (20 mL) and brine (10 mL). The

Table 4
Inhibitory activities (IC_{50}) of selected inhibitors.

Entry no.	IC_{50} (μM)
25c	21.0
26b	43.0
26h	24.0
26m	10.0
26n	14.0

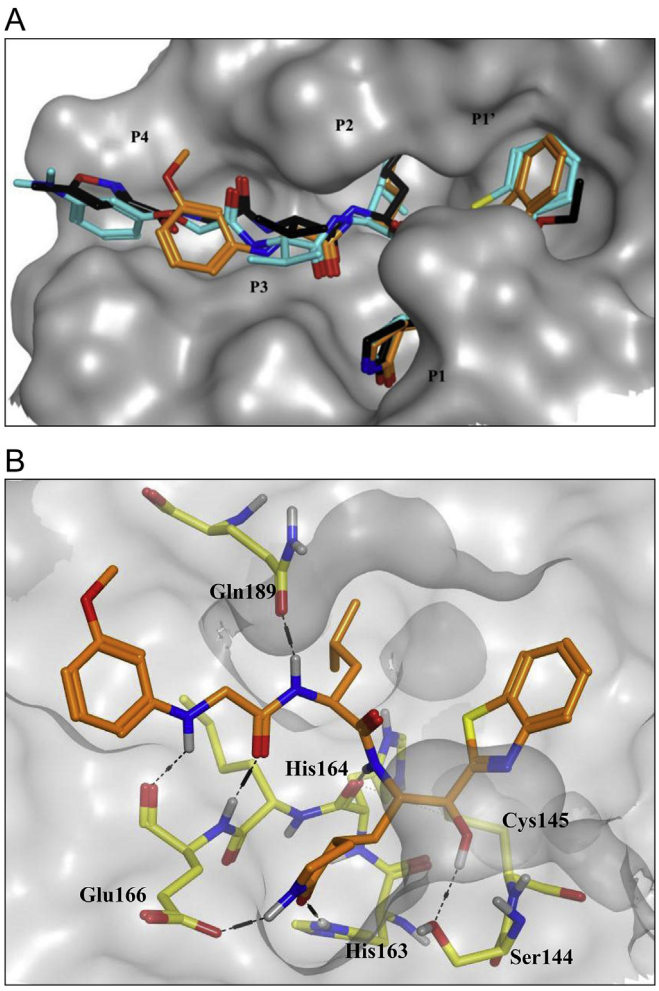

Fig. 2. Molecular dynamics stimulated pose of compound **26m** (orange stick) bound to SARS-CoV 3CL^{pro} (PDB ID: 1WOF (black stick)). (A) Overlapped view of **26m** with an original vinyl ester (black stick) and lead **9** (light blue stick); (B) compound **26m** was shown as an orange stick. Dotted black lines represent the hydrogen bonding interaction. A notable hydrogen bonding interaction between the amino group (–NH) of *N*-(3-methoxyphenyl)glycyl of **26m** with a backbone amino acid residue Glu166 of 3CL^{pro}.

resulting solution was dried over Na_2SO_4, filtered, and evaporated under reduced pressure to give compound **19b**, which was purified by silica gel column chromatography using hexane–EtOAc as eluents. Yield 85%; colorless oil; ^{1}H NMR (400 MHz, $CDCl_3$): δ 7.35–7.28 (m, 5H, merged with $CDCl_3$), 5.10 (s, 2H), 4.29–4.23 (m, 1H), 1.74–1.67 (m, 2H), 1.62–1.58 (m, 1H), 1.44 (s, 9H), 0.95–0.93 (m, 6H). HRMS (ESI): *m/z* calcd for $C_{18}H_{27}NO_4Na$ $[M + Na]^+$ 344.1838, found 344.1848.

The intermediates **19c–g** were prepared from benzyloxycarbonyl chloride and various commercially available amino acid esters **18b–f** according to the procedure described for the synthesis of **19c**.

4.2.3. Benzyl (S)-1-(methoxycarbonyl)pentylcarbamate (19c)

Yield 67% from L-norleucine methyl ester (**18b**); colorless oil; ^{1}H NMR (400 MHz, $CDCl_3$): δ 7.36–7.29 (m, 5H), 5.11 (s, 2H), 4.39–4.34 (q, J = 5.6 Hz, 1H), 3.73 (s, 3H), 1.88–1.79 (m, 1H), 1.66–1.63 (m, 1H), 1.38–1.33 (m, 4H), 0.90–0.87 (t, J = 6.4 Hz, 3H). HRMS (ESI): *m/z* calcd for $C_{15}H_{22}NO_4$ $[M + H]^+$ 280.1549, found 280.1545.

4.2.4. Benzyl (S)-1-(tert-butoxycarbonyl)-2-methylpropylcarbamate (19d)

Yield 71% from L-valine *tert*-butyl ester (**18c**); colorless oil; ^{1}H NMR (400 MHz, $CDCl_3$): δ 7.39–7.31 (m, 5H), 5.10 (s, 2H), 4.20–4.17 (m, 1H), 2.15–2.12 (m, 1H), 1.46 (s, 9H), 0.96–0.87 (m, 6H). HRMS (ESI): *m/z* calcd for $C_{17}H_{25}NO_4Na$ $[M + Na]^+$ 330.1681, found 330.1683.

4.2.5. Benzyl (1S,2R)-1-(tert-butoxycarbonyl)-2-methylbutylcarbamate (19e)

Yield 66% from L-isoleucine *tert*-butyl ester (**18d**); colorless oil; ^{1}H NMR (400 MHz, $CDCl_3$): δ 7.36–7.29 (m, 5H), 5.30–5.28 (m, NH, 1H), 5.17 (s, 2H), 4.25–4.20 (m, 1H), 1.85–1.80 (m, 1H), 1.44 (s, 9H), 1.21–1.01 (m, 2H), 0.94–0.91 (m, 6H). HRMS (ESI): *m/z* calcd for $C_{18}H_{28}NO_4$ $[M + H]^+$ 322.2018, found 322.2010.

4.2.6. Benzyl (S)-1-(tert-butoxycarbonyl)-3-(methylthio)propylcarbamate (19f)

Yield 72% from L-methionine *tert*-butyl ester (**18e**); colorless oil; δ 7.36–7.28 (m, 5H), 5.10 (s, 2H), 4.36 (q, J = 6.0 Hz, 1H), 2.54–2.46 (m, 2H), 2.08 (m, 5H), 1.94–1.92 (m, 2H), 1.46 (s, 9H). HRMS (ESI): *m/z* calcd for $C_{17}H_{26}NO_4S$ $[M + H]^+$ 340.1583, found 340.1580.

4.2.7. Benzyl (S)-1-(methoxycarbonyl)-2-phenylethylcarbamate (19g)

Yield 82% from L-phenylalanine methyl ester (**18f**): colorless solid; ^{1}H NMR (400 MHz, $CDCl_3$): δ 7.36–7.31 (m, 4H), 7.29–7.21 (m, 3H), 7.10–7.07 (m, 3H), 5.09 (s, 2H), 4.68–4.63 (m, 1H), 3.70 (s, 3H), 3.16–3.04 (m, 2H). HRMS (ESI): *m/z* calcd for $C_{18}H_{19}NO_4Na$ $[M + Na]^+$ 336.1212, found 336.1224.

4.2.8. (S)-tert-Butyl 2-(2-phenylacetamido)-4-methylpentanoate (19h)

Yield 59% from L-leucine *tert*-butyl ester (**18a**); colorless solid; ^{1}H NMR (400 MHz, $CDCl_3$): δ 7.35 (t, J = 7.6 Hz, 2H), 7.31–7.28 (m, 3H, merged with $CDCl_3$), 4.52–4.47 (m, 1H), 3.59 (s, 2H), 1.57–1.52 (m, 3H), 1.42 (s, 9H), 0.88 (d, J = 4.8 Hz, 6H). HRMS (ESI): *m/z* calcd for $C_{18}H_{28}NO_3$ $[M + H]^+$ 306.2069, found 306.2065.

4.2.9. (S)-tert-Butyl 2-(2-(4-methoxyphenyl)acetamido)-4-methylpentanoate (19i)

Yield 69% from L-leucine *tert*-butyl ester (**18a**); colorless solid; ^{1}H NMR (400 MHz, $CDCl_3$): δ 7.17 (d, J = 8.4 Hz, 2H), 6.87 (d, J = 8.0 Hz, 2H), 4.51–4.46 (m, 1H), 3.79 (s, 3H), 3.53 (s, 2H), 1.57–1.52 (m, 3H), 1.42 (s, 9H), 0.88–0.87 (m, 6H). HRMS (ESI): *m/z* calcd for $C_{19}H_{27}NO_4$ $[M + H]^+$ 336.2175, found 336.2173.

4.2.10. (S)-tert-Butyl 2-(3-(4-methoxyphenyl)propanamido)-4-methylpentanoate (19j)

Yield 79% from L-leucine *tert*-butyl ester (**18a**); colorless oil; ^{1}H NMR (400 MHz, $CDCl_3$): δ 7.13 (d, J = 8.8 Hz, 2H), 6.83 (d, J = 8.0 Hz, 2H), 4.54–4.48 (m, 1H), 3.79 (s, 3H), 2.94–2.90 (m, 2H), 2.55–2.44 (m, 2H), 1.56–1.44 (m, 3H), 1.44 (s, 9H), 0.90–0.88 (m, 6H). HRMS (ESI): *m/z* calcd for $C_{20}H_{31}NO_4Na$ $[M + Na]^+$ 372.2151, found 372.2145.

4.2.11. (S)-tert-Butyl 2-(3-(pyridin-3-yl)propanamido)-4-methylpentanoate (19k)

Yield 56% from L-leucine *tert*-butyl ester (**18a**); yellow oil; ^{1}H NMR (400 MHz, $CDCl_3$): δ 8.52 (s, 1H), 8.46 (d, J = 3.6 Hz, 1H), 7.74–7.69 (t, J = 8.0 Hz, 1H), 7.32–7.28 (m, 1H), 4.52–4.47 (m, 1H), 3.05–3.01 (m, 2H), 2.62–2.52 (m, 2H), 1.58–1.48 (m, 3H), 1.46 (s, 9H), 0.91–0.89 (m, 6H). HRMS (ESI): *m/z* calcd for $C_{18}H_{29}N_2O_3$ $[M + H]^+$ 321.2178, found 321.2188.

4.2.12. (S)-tert-Butyl 2-(cinnamamido)-4-methylpentanoate (19l)

Yield 79% from L-leucine *tert*-butyl ester (**18a**); colorless oil; ^{1}H NMR (400 MHz, CD_3OD): δ 7.44 (d, J = 21.0 Hz, 1H), 7.41 (d, J = 7.4 Hz, 2H), 7.29–7.26 (m, 5H), 6.58 (d, J = 21.0 Hz, 1H), 4.40–4.30 (m, 1H), 1.86–1.50 (m, 3H), 1.36 (s, 9H), 0.95–0.79 (m, 6H). HRMS (ESI): *m/z* calcd for $C_{19}H_{28}NO_3$ $[M + H]^+$ 318.2069, found 318.2077.

4.2.13. (S)-tert-Butyl 2-((E)-3-(4-methoxyphenyl)acrylamido)-4-methylpentanoate (19m)

Yield 76% from L-leucine *tert*-butyl ester (**18a**); colorless oil; ^{1}H NMR (400 MHz, $CDCl_3$): δ 7.58 (d, J = 15.6 Hz, 1H), 7.44 (d, J = 8.6 Hz, 2H), 6.88 (d, J = 8.6 Hz, 1H), 6.29 (d, J = 15.6 Hz, 1H), 4.70–4.65 (m, 1H), 3.89 (s, 3H), 1.73–1.48 (m, 3H), 1.43 (s, 9H), 0.98–0.95 (m, 6H). HRMS (ESI): *m/z* calcd for $C_{20}H_{31}NO_4$ $[M + H]^+$ 348.2175, found 348.2183.

4.2.14. (S)-tert-Butyl 2-((E)-3-(3,4-dimethoxyphenyl)acrylamido)-4-methylpentanoate (19n)

Yield 69% from L-leucine *tert*-butyl ester (**18a**); colorless oil; ^{1}H NMR (400 MHz, $CDCl_3$): δ 7.53 (d, J = 15.6 Hz, 1H), 7.04 (d, J = 8.0 Hz, 1H), 7.00 (s, 1H), 6.84 (d, J = 8.0 Hz, 1H), 6.30 (d, J = 15.6 Hz, 1H), 4.71–4.65 (m, 1H), 3.90 (s, 6H), 1.74–1.49 (m, 3H), 1.43 (s, 9H), 0.98–0.95 (m, 6H). HRMS (ESI): *m/z* calcd for $C_{21}H_{33}NO_5$ $[M + H]^+$ 378.2280, found 378.2282.

4.2.15. (S)-tert-Butyl 2-(2-phenoxyacetamido)-4-methylpentanoate (19o)

Yield 77% from L-leucine *tert*-butyl ester (**18a**); colorless oil; ^{1}H NMR (400 MHz, $CDCl_3$): δ 7.33 (t, J = 8.4 Hz, 2H), 7.03 (t, J = 8.0 Hz, 1H), 6.96 (d, J = 8.0 Hz, 2H), 4.63–4.60 (m, 1H), 4.52 (s, 2H), 1.68–1.54 (m, 3H), 1.47 (s, 9H), 0.96–0.94 (m, 6H). HRMS (ESI): *m/z* calcd for $C_{18}H_{27}NO_4Na$ $[M + Na]^+$ 344.1838, found 344.1835.

4.2.16. (S)-tert-Butyl 2-(2-(4-methoxyphenoxy)acetamido)-4-methylpentanoate (19p)

Yield 79% from L-leucine *tert*-butyl ester (**18a**); yellow oil; ^{1}H NMR (400 MHz, $CDCl_3$): δ 6.90–6.84 (m, 4H), 4.62–4.59 (m, 1H), 4.46 (s, 2H), 3.78 (s, 3H), 1.68–1.54 (m, 3H), 1.47 (s, 9H), 0.96–0.94 (m, 6H). HRMS (ESI): *m/z* calcd for $C_{18}H_{29}NO_4Na$ $[M + Na]^+$ 374.1943, found 374.1953.

4.2.17. (S)-tert-Butyl 2-(2-(4-hydroxyphenoxy)acetamido)-4-methylpentanoate (19q)

Yield 63% from L-leucine *tert*-butyl ester (**18a**); colorless solid; ^{1}H NMR (400 MHz, CD_3OD): δ 6.75–6.72 (m, 2H), 6.63–6.60 (m, 2H), 4.36 (s, 2H), 4.32–4.29 (m, 1H), 1.56–1.50 (m, 3H), 1.35 (s, 9H),

0.84–0.78 (m, 6H). HRMS (ESI): *m/z* calcd for $C_{18}H_{27}NO_5$ $[M + H]^+$ 338.1967, found 338.1961.

4.2.18. (S)-tert-Butyl 2-(2-(3-(dimethylamino)phenoxy)acetamido)-4-methylpentanoate (**19r**)

Yield 62% from L-leucine *tert*-butyl ester (**18a**); yellow solid; ^1H NMR (400 MHz, $CDCl_3$): δ 7.17 (t, $J = 8.0$ Hz, 1H), 6.97 (d, $J = 8.0$ Hz, 1H), 6.43 (d, $J = 8.0$ Hz, 1H), 6.32 (s, 1H), 4.66–4.61 (m, 1H), 4.52 (s, 2H), 2.85 (s, 6H), 1.68–1.55 (m, 3H), 1.46 (s, 9H), 0.97–0.94 (m, 6H). HRMS (ESI): *m/z* calcd for $C_{20}H_{33}N_2O_4$ $[M + H]^+$ 365.2440, found 365.2430.

4.2.19. (S)-tert-Butyl 2-(2-((4-methoxyphenyl)amino)acetamido)-4-methylpentanoate (**19s**)

Yield 54% from L-leucine *tert*-butyl ester (**18a**); brown viscous oil; ^1H NMR (400 MHz, $CDCl_3$): δ 6.78 (d, $J = 8.0$ Hz, 2H), 6.58 (d, $J = 8.0$ Hz, 1H), 4.56–4.49 (m, 1H), 3.77–3.71 (m, 5H), 1.55–1.38 (m, 12H), 0.96–0.86 (m, 6H). HRMS (ESI): *m/z* calcd for $C_{19}H_{30}N_2O_4$ $[M + H]^+$ 351.2284, found 351.2279.

4.2.20. (S)-tert-Butyl 2-(2-((3-methoxyphenyl)amino)acetamido)-4-methylpentanoate (**19t**)

Yield 57% from L-leucine *tert*-butyl ester (**18a**); brown viscous oil; ^1H NMR (400 MHz, $CDCl_3$): δ 7.00 (d, $J = 8.0$ Hz, 1H), 6.87–6.85 (m, 2H), 6.77 (s, 1H), 4.58–4.53 (m, 1H), 3.89–3.71 (m, 5H), 1.57–1.51 (m, 2H), 1.48–1.46 (m, 1H), 1.43 (s, 9H), 0.95–0.91 (m, 6H). HRMS (ESI): *m/z* calcd for $C_{19}H_{30}N_2O_4$ $[M + H]^+$ 351.2284, found 351.2297.

4.2.21. (S)-tert-Butyl 2-(2-((2-methoxyphenyl)amino)acetamido)-4-methylpentanoate (**19u**)

Yield 60% from L-leucine *tert*-butyl ester (**18a**); light pink solid; ^1H NMR (400 MHz, $CDCl_3$): δ 6.87–6.74 (m, 3H), 6.51 (d, $J = 8.0$ Hz, 1H), 4.58–4.53 (m, 1H), 3.87–3.75 (s, 5H), 1.57–1.52 (m, 2H), 1.48–1.46 (m, 1H), 1.43 (s, 9H), 0.92–0.87 (m, 6H). HRMS (ESI): *m/z* calcd for $C_{19}H_{30}N_2O_4$ $[M + H]^+$ 351.2284, found 351.2277.

4.3. Synthetic procedure for the preparation of **20**

Procedure A: To a solution of the corresponding *tert*-butyl ester **19** (0.110 g, 0.31 mmol) in CH_2Cl_2 (2 mL) at 0 °C was added TFA/H_2O (10:1, 3 mL). After 5 min stirring, the reaction mixture was allowed to stir at room temperature for 1 h. The solvent was completely evaporated under reduced pressure to give the corresponding acids **20**, which were used directly in the subsequent step without further characterization.

Procedure B: To a solution of the corresponding methyl ester **19** (0.100 g, 0.35 mmol) in THF (3 mL) at room temperature was added LiOH in water (0.102 g, 2.45 mmol). After 3 h stirring, the solvent was completely evaporated under reduced pressure and the resulting residue was neutralized with 2 M HCl. The solution was extracted with EtOAc (20 mL × 2), dried over Na_2SO_4, filtered and evaporated under reduced pressure to give the corresponding acids **20**, which were directly used for next step without further characterizations.

4.4. Synthesis of tert-butyl (S)-1-(N-methoxy-N-methylcarbamoyl)-2-((S)-2-oxopyrrolidin-3-yl)ethylcarbamate (**23**)

Compound **22** was prepared through sequential reactions from the well-known intermediate **21**, as reported previously [20–22,31].

To a solution of **22** (3.27 g, 8.0 mmol) in methanol (5 mL) was added a 4 M NaOH solution (0.04 mol) at room temperature. The mixture was stirred for 4 h and the methanol was evaporated. The residue was neutralized with 2 M HCl and extracted with EtOAc (20 mL × 4). The organic layer was washed with brine, dried over Na_2SO_4, and evaporated under reduced pressure to yield the corresponding acid. To a solution of the acid (12.0 mmol) in DMF (30 mL) were added EDC·HCl (0.540 g, 10.0 mmol), HOBt·H_2O (0.330 g, 11.0 mmol), and *N*,*O*-dimethylhydroxylamine (0.213 g, 11.0 mmol) at ambient temperature. The solution was cooled to 0 °C, and TEA (0.240 mL, 11.0 mmol) was added slowly. After 2 h, the DMF was evaporated under high vacuum, and the resulting residue was dissolved in EtOAc (100 mL). The resulting solution was subsequently washed with 5% citric acid (20 mL × 2), 5% $NaHCO_3$ (20 mL × 2), and brine (50 mL). The organic layer was then dried over Na_2SO_4 and concentrated under reduced pressure to yield the Weinreb amide derivative **23**, which was purified by column chromatography (EtOAc/MeOH = 9.5:0.5).

The data for compounds **22** and **23** were reported previously [20,21].

4.4.1. tert-Butyl ((S)-1-(benzo[d]thiazol-2-yl)-1-oxo-3-((S)-2-oxo pyrrolidin-3-yl)propan-2-yl)carbamate (**24a**)

To a solution of benzothiazole (1.37 g, 10.0 mmol) in THF at −78 °C was added *n*-BuLi (2.0 M in THF, 1.67 mL) dropwise over 20 min. After 1 h stirring, the Weinreb amide **23** (0.064 g, 2.0 mmol) in THF was slowly added dropwise over 20 min and then the solution was stirred for 3 h at same temperature. The reaction was quenched with sat. NH_4Cl and allowed to stir at 0 °C for 20 min. The mixture was evaporated and dissolved in EtOAc. This solution was washed with water (100 mL) and brine (50 mL), and then dried over Na_2SO_4. After filtration, the organic layer was concentrated under reduced pressure and the resulting residue was subjected to flash chromatography (EtOAc/MeOH = 9:1) to obtain the pure compound **24a**. The data for the compound **24a** has been reported in a previous article [21].

4.4.2. tert-Butyl ((S)-1-oxo-3-((S)-2-oxopyrrolidin-3-yl)-1-(5-phenyl thiazol-2-yl)propan-2-yl)carbamate (**24b**)

To a cooled solution of the commercially available 5-phenylthiazole (0.175 g, 10 mmol) in dry THF at −78 °C was slowly added a solution of LDA (1.0 mL, 14 mmol). After 1 h, a pre-cooled solution containing the Weinreb amide **23** (0.329 g, 10 mmol) in anhydrous THF was slowly added, and the reaction was stirred at −78 °C over 2 h. The solution was allowed to warm to room temperature, was quenched by the addition of water (35 mL), and then extracted with EtOAc (3 × 50 mL). The combined organic layers were dried over anhydrous Na_2SO_4, filtered, and evaporated in vacuo. The crude mixture was then purified using flash chromatography (*n*-hexane/EtOAc = 3:7) to furnish **24b**. The data for the compound **24b** were reported previously [22].

Compounds **24c**–**e** were prepared from **23** according to the procedure described for the synthesis of **24b**.

4.4.3. tert-Butyl ((S)-1-oxo-3-((S)-2-oxopyrrolidin-3-yl)-1-(5-(p-tolyl) thiazol-2-yl)propan-2-yl)carbamate (**24c**)

The data for the compound **24c** has been reported in a previous article [22].

4.4.4. tert-Butyl ((S)-1-(5-(4-methoxyphenyl)thiazol-2-yl)-1-oxo-3-((S)-2-oxopyrrolidin-3-yl)propan-2-yl)carbamate (**24d**)

The data for the compound **24d** has been reported in a previous article [22].

4.4.5. tert-Butyl ((S)-1-(5-(4-methoxyphenyl)thiazol-2-yl)-1-oxo-3-((S)-2-oxopyrrolidin-3-yl)propan-2-yl)carbamate (**24e**)

The data for the compound **24e** has been reported in a previous article [22].

*4.5. Synthesis of (S)-N-((S)-1-(benzo[d]thiazol-2-yl)-1-oxo-3-((S)-2-oxopyrrolidin-3-yl)propan-2-yl)-4-methyl-2-(3-methylbutanamido) pentanamide (**25a**)*

To a solution of **24a** (0.200 g, 0.5 mmol) in CH_2Cl_2 (3 mL) at 0 °C was added TFA/H_2O (10:1, 5 mL), and the solution was stirred for 1 h. After evaporating the solvent under reduced pressure, the corresponding deprotected lactam residue (0.100 g, 0.53 mmol) was coupled to the carboxylic acid **20a** (0.136 g, 0.38 mmol) using the coupling agent HBTU (0.147 g, 0.38 mmol) in the presence of diisopropylethylamine (0.050 mL, 0.38 mmol) in DMF (3 mL) at 0 °C. The reaction mixture was allowed to stir for 2–3 h under ambient conditions. The solvent was then evaporated under a high vacuum, and the residue was dissolved in EtOAc (50 mL). The organic layer was washed with 5% citric acid (20 mL × 2), 5% $NaHCO_3$ (20 mL × 2), and brine (25 mL). This solution was dried over Na_2SO_4, filtered, and evaporated under reduced pressure to give compound **25a**. Yield 35%; light yellow solid; ^{1}H NMR (400 MHz, CD_3OD): δ 8.21 (d, J = 8.0 Hz, 1H), 8.11 (d, J = 8.0 Hz, 1H), 7.65–7.51 (m, 2H), 5.72–5.69 (m, 1H), 4.61–4.42 (m, 1H), 3.38–3.29 (m, 4H, merged with CD_3OD), 2.73–2.66 (m, 1H), 2.46–2.40 (m, 1H), 2.22–2.00 (m, 4H), 1.67–1.53 (m, 3H), 1.28–1.21 (m, 2H), 0.95–0.86 (m, 12H). ^{13}C NMR (400 MHz, CD_3OD): δ 193.3, 181.8, 175.8, 165.5, 154.8, 138.4, 129.3, 126.5, 123.7, 55.3, 53.1, 52.9, 46.1, 45.9, 41.8, 41.5, 40.0, 39.8, 29.4, 28.8, 27.5, 25.8, 23.4, 22.8, 21.9. HRMS (ESI): m/z calcd for $C_{25}H_{35}N_4O_4S$ $[M + H]^+$ 487.2379 found 487.2373.

Compounds **25b**–**h** were prepared from **24a** with **20a**–**h** using a procedure similar to that described for the synthesis of **25a**.

*4.5.1. tert-Butyl ((S)-1-(((S)-1-(benzo[d]thiazol-2-yl)-1-oxo-3-((S)-2-oxopyrrolidin-3-yl)propan-2-yl)amino)-4-methyl-1-oxopentan-2-yl)carbamate (**25b**)*

Yield 37% from **24a**; colorless solid; ^{1}H NMR (400 MHz, $CDCl_3$): δ 8.18 (d, J = 8.0 Hz, 1H), 7.99 (d, J = 7.6 Hz, 1H), 7.60–7.52 (m, 2H), 5.75–5.66 (m, 1H), 4.24–4.04 (m, 1H), 3.40–3.37 (m, 2H), 2.66–2.45 (m, 2H), 2.17–1.95 (m, 2H), 1.94–1.72 (m, 1H), 1.70–1.53 (m, 3H), 1.44 (s, 9H), 0.96–0.88 (m, 6H). HRMS (ESI): m/z calcd for $C_{25}H_{35}N_4O_5SNa$ $[M + Na]^+$ 525.2148, found 525.2145.

*4.5.2. Benzyl ((S)-1-(((S)-1-(benzo[d]thiazol-2-yl)-1-oxo-3-((S)-2-oxopyrrolidin-3-yl)propan-2-yl)amino)-4-methyl-1-oxopentan-2-yl) carbamate (**25c**)*

Yield 43% from **24a**; colorless solid; ^{1}H NMR (400 MHz, $CDCl_3$): δ 8.16 (d, J = 8.4 Hz, 1H), 7.97 (d, J = 8.4 Hz, 1H), 7.58–7.51 (m, 2H), 7.32–7.27 (m, 5H, merged with $CDCl_3$), 5.70–5.58 (m, 1H), 5.12–5.08 (m, 2H), 4.39–4.14 (m, 1H), 3.30–3.27 (m, 2H), 2.64–2.49 (m, 2H), 2.24–2.10 (m, 2H), 2.09–1.89 (m, 1H), 1.86–1.67 (m, 2H), 1.66–1.48 (m, 1H), 0.93–0.85 (m, 6H). ^{13}C NMR (400 MHz, CD_3OD): δ 193.5, 181.8, 175.8, 165.5, 158.4, 154.8, 138.4, 129.4, 128.7, 127.3, 126.5, 123.7, 67.7, 67.5, 56.0, 55.1, 54.9, 42.0, 41.9, 39.9, 33.9, 32.7, 29.3, 28.7, 25.8, 23.7, 22.0, 21.8. HRMS (ESI): m/z calcd for $C_{28}H_{33}N_4O_5S$ $[M + H]^+$ 537.2172 found 537.2153.

*4.5.3. Benzyl ((S)-1-(((S)-1-(benzo[d]thiazol-2-yl)-1-oxo-3-((S)-2-oxopyrrolidin-3-yl)propan-2-yl)amino)-1-oxohexan-2-yl)carbamate (**25d**)*

Yield 45% from **24a**; light yellow solid; ^{1}H NMR (400 MHz, CD_3OD): δ 8.37–8.28 (m, 2H), 7.69–7.64 (m, 2H), 7.40–7.30 (m, 5H), 5.56–5.47 (m, 1H), 5.04–4.99 (m, 2H), 4.07–4.01 (m, 1H), 3.22–3.11 (m, 2H, merged with CD_3OD), 2.51–2.11 (m, 3H), 1.97–1.75 (m, 2H), 1.67–1.49 (m, 2H), 1.21–1.08 (m, 4H), 0.85–0.72 (m, 3H). ^{13}C NMR (400 MHz, CD_3OD): δ 202.2, 192.8, 178.0, 172.4, 164.3, 155.8, 152.8, 137.0, 136.3, 77.2, 65.2, 64.2, 42.1, 41.9, 41.5, 37.8, 36.6, 32.0, 31.6, 31.5, 28.1, 27.4, 25.9, 23.6, 21.7, 21.5, 13.6. HRMS (ESI): m/z calcd for $C_{28}H_{33}N_4O_5S$ $[M + H]^+$ 537.2172 found 537.2166.

*4.5.4. Benzyl ((S)-1-(((S)-1-(benzo[d]thiazol-2-yl)-1-oxo-3-((S)-2-oxopyrrolidin-3-yl)propan-2-yl)amino)-3-methyl-1-oxobutan-2-yl) carbamate (**25e**)*

Yield 39% from **24a**; yellow solid; ^{1}H NMR (400 MHz, $CDCl_3$): δ 8.18 (d, J = 8.0 Hz, 1H), 7.98 (d, J = 8.0 Hz, 1H), 7.59–7.51 (m, 2H), 7.39–7.30 (m, 5H), 5.74–5.65 (m, 1H), 5.15–5.09 (m, 2H), 4.40–4.20 (m, 1H), 3.39–3.36 (m, 2H), 2.65–2.52 (m, 2H), 2.30–2.16 (m, 3H), 2.03–1.96 (m, 1H), 1.10–0.89 (m, 6H). ^{13}C NMR (400 MHz, CD_3OD): δ 193.5, 181.8, 174.6, 165.4, 158.5, 154.7, 138.4, 129.5, 129.0, 128.7, 126.6, 123.7, 79.5, 78.9, 67.6, 61.1, 55.3, 41.6, 40.0, 38.2, 38.1, 33.9, 33.2, 32.7, 28.7, 25.9, 23.7. HRMS (ESI): m/z calcd for $C_{27}H_{31}N_4O_5S$ $[M + H]^+$ 523.2015 found 523.2003.

*4.5.5. Benzyl ((2S,3R)-1-(((S)-1-(benzo[d]thiazol-2-yl)-1-oxo-3-((S)-2-oxopyrrolidin-3-yl)propan-2-yl)amino)-3-methyl-1-oxopentan-2-yl)carbamate (**25f**)*

Yield 42% from **24a**; light yellow solid; ^{1}H NMR (400 MHz, CD_3OD): δ 8.19 (d, J = 8.4 Hz, 1H), 8.08 (d, J = 8.4 Hz, 1H), 7.63–7.56 (m, 2H), 7.33–7.27 (m, 5H), 5.75–5.73 (m, 1H), 5.11–5.03 (s, 2H), 4.12–4.05 (m, 1H), 3.35–3.25 (m, 2H, merged with CD_3OD), 2.70–2.50 (m, 1H), 2.49–2.39 (m, 1H), 2.38–2.01 (m, 2H), 2.00–1.85 (m, 1H), 1.80–1.75 (m, 1H), 1.67–1.49 (m, 2H), 1.08–0.86 (m, 6H). HRMS (ESI): m/z calcd for $C_{28}H_{33}N_4O_5S$ $[M + H]^+$ 537.2178 found 537.2178.

*4.5.6. Benzyl ((S)-1-(((S)-1-(benzo[d]thiazol-2-yl)-1-oxo-3-((S)-2-oxopyrrolidin-3-yl)propan-2-yl)amino)-4-(methylthio)-1-oxobutan-2-yl)carbamate (**25g**)*

Yield 45% from **24a**; white solid; ^{1}H NMR (400 MHz, $CDCl_3$): δ 8.19 (d, J = 8.4 Hz, 1H), 8.00 (d, J = 8.0 Hz, 1H), 7.59–7.52 (m, 2H), 7.35–7.25 (m, 5H), 5.78–5.61 (m, 1H), 5.20–5.10 (m, 2H), 4.60–4.44 (m, 1H), 3.40–3.34 (m, 2H), 2.69–2.50 (m, 1H), 2.49–2.38 (m, 2H), 2.38–2.09 (m, 2H), 2.08–2.00 (m, 5H), 1.99–1.89 (m, 2H). ^{13}C NMR (400 MHz, CD_3OD): δ 193.5, 181.8, 174.8, 165.7, 165.4, 158.4, 154.7, 138.4, 129.4, 129.3, 128.8, 127.3, 126.5, 123.7, 67.8, 56.0, 41.5, 40.0, 33.8, 32.8, 31.7, 31.0, 30.7, 29.3, 28.7, 24.1, 15.2. HRMS (ESI): m/z calcd for $C_{27}H_{31}N_4O_5S_2$ $[M + H]^+$ 555.1736 found 555.1743.

*4.5.7. Benzyl ((S)-1-(((S)-1-(benzo[d]thiazol-2-yl)-1-oxo-3-((S)-2-oxopyrrolidin-3-yl)propan-2-yl)amino)-1-oxo-3-phenylpropan-2-yl)carbamate (**25h**)*

Yield 43% from **24a**; colorless solid; ^{1}H NMR (400 MHz, $CDCl_3$): δ 8.19 (d, J = 7.6 Hz, 1H), 7.99 (d, J = 7.6 Hz, 1H), 7.61–7.55 (m, 2H), 7.51–7.17 (m, 10H, merged with $CDCl_3$), 5.82–5.79 (m, 1H), 5.11–5.08 (m, 2H), 4.43–4.30 (m, 1H), 3.39–3.31 (m, 2H), 3.20–3.15 (m, 2H), 2.65–2.45 (m, 2H), 2.39–2.14 (m, 3H). ^{13}C NMR (400 MHz, $CDCl_3$): δ 192.9, 181.2, 174.3, 165.6, 163.8, 161.8, 154.8, 141.9, 139.2, 129.3, 128.9, 127.4, 127.0, 126.2, 125.9, 125.5, 123.3, 117.9, 114.1, 63.1, 55.2, 54.4, 41.6, 44.3, 41.4, 39.7, 38.2, 33.0, 27.8, 24.7, 22.8. HRMS (ESI): m/z calcd for $C_{31}H_{32}N_4O_5S$ $[M + H]^+$ 571.2015 found 571.2003.

*4.6. Synthesis of **26***

Compounds **26a**–**r** were prepared from **24a** with **20i**–**u** using a procedure similar to that described for the synthesis of **25a**.

*4.6.1. (S)-N-((S)-1-(Benzo[d]thiazol-2-yl)-1-oxo-3-((S)-2-oxopyrrolidin-3-yl)propan-2-yl)-4-methyl-2-(2-phenylacetamido) pentanamide (**26a**)*

Yield 47% from **24a**; white solid; ^{1}H NMR (400 MHz, CD_3OD): δ 8.09 (d, J = 8.0 Hz, 1H), 8.01 (d, J = 8.0 Hz, 1H), 7.55–7.47 (m, 2H), 7.19–7.11 (m, 5H), 5.61–5.57 (m, 1H), 4.35–4.32 (m, 1H), 3.44 (s, 2H), 3.40–3.36 (m, 1H), 3.19–3.07 (m, 1H), 2.57–2.52 (m, 1H),

2.39–2.20 (m, 2H), 2.12–1.88 (m, 2H), 1.79–1.48 (m, 3H), 0.88–0.76 (m, 6H). ^{13}C NMR (400 MHz, CD_3OD): δ 193.5, 181.8, 175.1, 165.5, 154.8, 138.4, 136.9, 130.2, 129.5, 128.4, 127.8, 126.5, 124.2, 123.7, 55.9, 55.2, 53.3, 43.7, 41.8, 39.9, 39.2, 33.7, 32.8, 29.4, 28.7, 25.8, 23.7, 22.1. HRMS (ESI): *m/z* calcd for $C_{28}H_{33}N_4O_4S$ $[M + H]^+$ 521.2223 found 521.2216.

*4.6.2. (S)-N-((S)-1-(Benzo[d]thiazol-2-yl)-1-oxo-3-((S)-2-oxopyrro lidin-3-yl)propan-2-yl)-2-(2-(4-methoxyphenyl)acetamido)-4-methylpentanamide (**26b**)*

Yield 37% from **24a**; yellow solid; ^{1}H NMR (400 MHz, CD_3OD): δ 8.20 (d, *J* = 8.0 Hz, 1H), 8.11 (d, *J* = 8.0 Hz, 1H), 7.64–7.58 (m, 2H), 7.20 (d, *J* = 8.0 Hz, 2H), 6.84 (d, *J* = 8.4 Hz, 2H), 5.69–5.67 (m, 1H), 4.45–4.41 (m, 1H), 3.73 (s, 3H), 3.51–3.21 (m, 4H, merged with CD_3OD), 2.63–2.52 (m, 1H), 2.51–2.21 (m, 2H), 2.10–1.88 (m, 2H), 1.86–1.55 (m, 3H), 0.92–0.81 (m, 6H). ^{13}C NMR (400 MHz, CD_3OD): δ 193.5, 181.8, 175.1, 174.4, 165.5, 160.1, 154.8, 138.4, 131.4, 129.3, 128.4, 126.5, 123.7, 114.9, 55.6, 55.2, 42.8, 42.6, 41.6, 41.5, 39.9, 33.7, 29.4, 28.7, 25.8, 25.4, 24.2, 23.2, 22.1. HRMS (ESI): *m/z* calcd for $C_{29}H_{34}N_4O_5SNa$ $[M + Na]^+$ 573.2148 found 573.2148.

*4.6.3. (S)-N-((S)-1-(Benzo[d]thiazol-2-yl)-1-oxo-3-((S)-2-oxopyrro lidin-3-yl)propan-2-yl)-2-(3-(4-methoxyphenyl)propanamido)-4-methylpentanamide (**26c**)*

Yield 43% from **24a**; colorless solid; ^{1}H NMR (400 MHz, $CDCl_3$): δ 8.17 (d, *J* = 8.4 Hz, 1H), 7.98 (d, *J* = 8.0 Hz, 1H), 7.60–7.51 (m, 2H), 7.10 (d, *J* = 8.4 Hz, 2H), 6.81 (d, *J* = 8.4 Hz, 2H), 5.67–5.55 (m, 1H), 4.59–4.50 (m, 1H), 3.79 (s, 3H), 3.40–3.37 (m, 2H), 2.93–2.89 (m, 2H), 2.66–2.43 (m, 4H), 2.22–1.99 (m, 3H), 1.77–1.57 (m, 2H), 1.46–1.40 (m, 1H), 0.91–0.86 (m, 6H). ^{13}C NMR (400 MHz, $CDCl_3$): δ 192.2, 180.3, 172.2, 162.9, 162.5, 158.0, 155.7, 155.4, 147.6, 140.6, 132.7, 129.7, 129.3, 127.3, 113.8, 55.2, 54.8, 50.0, 41.5, 40.6, 38.6, 38.4, 34.8, 33.4, 30.0, 28.7, 27.9, 24.7, 22.8, 21.9. HRMS (ESI): *m/z* calcd for $C_{30}H_{36}N_4O_5SNa$ $[M + Na]^+$ 587.2034 found 587.2032.

*4.6.4. (S)-N-((S)-1-(Benzo[d]thiazol-2-yl)-1-oxo-3-((S)-2-oxopyrro lidin-3-yl)propan-2-yl)-4-methyl-2-(3-(pyridin-3-yl)propanamido) pentanamide (**26d**)*

Yield 27% from **24a**; brown solid; ^{1}H NMR (400 MHz, $CDCl_3$): δ 8.30–8.28 (m, 2H), 7.88–7.86 (d, *J* = 8.0 Hz, 1H), 7.66–7.64 (m, 2H), 7.51–7.26 (m, 2H), 7.20–7.16 (m, 1H), 5.61–5.57 (m, 1H), 4.49–4.45 (m, 1H), 3.35–3.29 (m, 2H), 3.01–2.97 (m, 2H), 2.83–2.80 (m, 2H), 2.71–2.69 (m, 2H), 2.58–2.42 (m, 3H), 2.41–2.25 (m, 2H), 1.90–1.84 (m, 1H), 1.73–1.53 (m, 2H), 0.96–0.85 (m, 6H). HRMS (ESI): *m/z* calcd for $C_{28}H_{34}N_5O_4S$ $[M + H]^+$ 536.2332 found 536.2327.

*4.6.5. (S)-N-((S)-1-(Benzo[d]thiazol-2-yl)-1-oxo-3-((S)-2-oxopyrro lidin-3-yl)propan-2-yl)-2-cinnamamido-4-methylpentanamide (**26e**)*

Yield 41% from **24a**; yellow solid; ^{1}H NMR (400 MHz, $CDCl_3$): δ 8.17–8.15 (m, *J* = 8.0 Hz, 1H), 7.97–7.93 (m, 1H), 7.70–7.50 (m, 5H), 7.49–7.45 (m, 2H), 6.47–6.43 (m, 1H), 5.70–5.60 (m, 1H), 4.90–4.72 (m, 1H), 3.40–3.27 (m, 2H), 2.60–2.45 (m, 2H), 2.40–1.99 (m, 2H), 1.95–1.80 (m, 1H), 1.76–1.42 (m, 3H), 0.96–0.83 (m, 6H). ^{13}C NMR (400 MHz, CD_3OD): δ 193.5, 181.2, 176.3, 165.7, 154.7, 142.4, 138.3, 136.2, 130.9, 129.9, 128.4, 126.5, 123.7, 121.3, 56.1, 55.6, 54.4, 53.7, 42.1, 41.6, 40.1, 33.8, 30.7, 29.52, 28.9, 26.0, 25.9, 23.3, 22.1. HRMS (ESI): *m/z* calcd for $C_{29}H_{33}N_4O_4S$ $[M + H]^+$ 533.2223 found 533.2243.

*4.6.6. (S)-N-((S)-1-(Benzo[d]thiazol-2-yl)-1-oxo-3-((S)-2-oxopyrro lidin-3-yl)propan-2-yl)-2-((E)-3-(4-methoxyphenyl)acrylamido)-4-methylpentanamide (**26f**)*

Yield 33% from **24a**; yellow solid; ^{1}H NMR (400 MHz, CD_3OD): δ 8.26 (d, *J* = 7.0 Hz, 1H), 8.18–8.10 (m, 1H), 7.70–7.55 (m, 2H), 7.54–7.42 (m, 3H), 6.95 (d, *J* = 8.8 Hz, 2H), 6.90–6.88 (m, 1H), 6.61–6.50 (m, 2H), 5.80–5.62 (m, 1H), 4.62–4.50 (m, 1H), 3.84 (s, 3H), 3.40–3.29 (m, 2H, merged with CD_3OD), 2.80–2.65 (m, 1H), 2.63–2.45 (m, 1H), 2.43–2.20 (m, 1H), 2.19–1.99 (m, 1H), 1.92–1.78 (m, 1H), 1.77–1.50 (m, 3H), 1.05–0.88 (m, 6H). ^{13}C NMR (400 MHz, CD_3OD): δ 191.9, 180.2, 173.3, 166.6, 163.7, 160.8, 153.2, 140.9, 137.1, 129.3, 127.9, 127.4, 127.0, 125.5, 122.3, 117.9, 117.7, 114.1, 55.2, 54.4, 51.6, 51.4, 41.6, 40.4, 38.7, 33.0, 27.6, 24.6, 22.7, 21.6. HRMS (ESI): *m/z* calcd for $C_{30}H_{34}N_4O_5S$ $[M + H]^+$ 563.2328 found 563.2328.

*4.6.7. (S)-N-((S)-1-(Benzo[d]thiazol-2-yl)-1-oxo-3-((S)-2-oxopyrro lidin-3-yl)propan-2-yl)-2-((E)-3-(3,4-dimethoxyphenyl)acrylamido)-4-methylpentanamide (**26g**)*

Yield 42% from **24a**; yellow solid; ^{1}H NMR (400 MHz, $CDCl_3$): δ 8.20–8.14 (m, 1H), 8.00–7.94 (m, 1H), 7.60–7.50 (m, 3H), 7.10–6.99 (m, 2H), 6.84 (d, *J* = 8.0 Hz, 1H), 6.30 (d, *J* = 16.0 Hz, 1H), 5.85–5.60 (m, 1H), 4.78–4.66 (m, 1H), 3.90 (s, 6H), 3.42–3.30 (m, 2H), 2.70–2.45 (m, 2H), 2.40–2.25 (m, 2H), 2.20–1.85 (m, 2H), 1.80–1.64 (m, 2H), 1.10–0.88 (m, 6H). ^{13}C NMR (400 MHz, CD_3OD): δ 193.5, 182.4, 176.2, 169.7, 155.5, 152.3, 149.5, 142.8, 138.3, 135.3, 131.9, 129.3, 127.3, 125.7, 123.5, 119.3, 112.7, 117.7, 56.5, 54.2, 53.6, 42.3, 41.6, 40.0, 33.8, 30.7, 29.3, 28.8, 25.8, 23.6, 22.1. HRMS (ESI): *m/z* calcd for $C_{31}H_{36}N_4O_6SNa$ $[M + Na]^+$ 615.2253 found 615.2253.

*4.6.8. (S)-N-((S)-1-(Benzo[d]thiazol-2-yl)-1-oxo-3-((S)-2-oxopyrro lidin-3-yl)propan-2-yl)-4-methyl-2-(2-phenoxyacetamido)pentana mide (**26h**)*

Yield 45% from **24a**; colorless solid; ^{1}H NMR (400 MHz, $CDCl_3$): δ 8.17 (d, *J* = 8.0 Hz, 1H), 8.00–7.97 (m, 1H), 7.60–7.51 (m, 2H), 7.31–7.27 (m, 2H, merged with $CDCl_3$), 7.10–6.85 (m, 3H), 5.70–5.65 (m, 1H), 4.76–4.66 (m, 1H), 4.55–4.50 (m, 2H), 3.40–3.21 (m, 2H), 2.70–2.50 (m, 2H), 2.35–2.19 (m, 1H), 2.34–2.20 (m, 2H), 2.19–1.85 (m, 1H), 1.80–1.65 (m, 2H), 1.00–0.88 (m, 6H). ^{13}C NMR (400 MHz, CD_3OD): δ 193.6, 181.8, 174.8, 174.5, 171.5, 165.5, 159.2, 154.7, 138.4, 130.6, 129.3, 126.7, 123.7, 115.8, 68.1, 55.9, 52.9, 41.9, 40.7, 39.8, 33.7, 29.2, 28.8, 25.7, 23.5, 22.0, 21.7, 21.2. HRMS (ESI): *m/z* calcd for $C_{28}H_{33}N_4O_5S$ $[M + H]^+$ 537.2174 found 537.2174.

*4.6.9. (S)-N-((S)-1-(Benzo[d]thiazol-2-yl)-1-oxo-3-((S)-2-oxopyrro lidin-3-yl)propan-2-yl)-2-(2-(4-methoxyphenoxy)acetamido)-4-methylpentanamide (**26i**)*

Yield 45% from **24a**; yellow solid; ^{1}H NMR (400 MHz, $CDCl_3$): δ 8.18 (d, *J* = 7.6 Hz, 1H), 7.99 (d, *J* = 7.6 Hz, 1H), 7.60–7.52 (m, 2H), 6.90–6.80 (m, 4H), 5.81–5.65 (m, 1H), 4.70–4.61 (m, 1H), 4.60–4.45 (m, 2H), 3.76 (s, 3H), 3.40–3.28 (m, 2H), 2.75–2.40 (m, 2H), 2.39–1.90 (m, 3H), 1.89–1.58 (m, 3H), 1.00–0.89 (m, 6H). ^{13}C NMR (400 MHz, CD_3OD): δ 192.5, 180.2, 172.4, 169.4, 168.7, 163.8, 154.7, 151.5, 145.3, 137.2, 128.0, 127.1, 125.6, 122.4, 115.9, 114.7, 68.1, 55.6, 53.8, 41.7, 40.6, 38.0, 37.8, 32.9, 28.8, 25.8, 23.5, 22.0, 21.8. HRMS (ESI): *m/z* calcd for $C_{29}H_{35}N_4O_6S$ $[M + H]^+$ 567.2277, found 567.2268.

*4.6.10. (S)-N-((S)-1-(Benzo[d]thiazol-2-yl)-1-oxo-3-((S)-2-oxopyr rolidin-3-yl)propan-2-yl)-2-(2-(4-hydroxyphenoxy)acetamido)-4-methylpentanamide (**26j**)*

Yield 40% from **24a**; yellow solid; ^{1}H NMR (400 MHz, CD_3OD): δ 8.21 (d, *J* = 8.1 Hz, 1H), 8.11 (d, *J* = 8.1 Hz, 1H), 7.65–7.58 (m, 2H), 6.82–6.78 (m, 2H), 6.70–6.65 (m, 2H), 5.78–5.66 (m, 1H), 4.55–4.50 (m, 1H), 4.60–4.45 (m, 2H), 3.35–3.18 (m, 2H, merged with CD_3OD) 2.75–2.45 (m, 1H), 2.44–2.20 (m, 2H), 2.19–1.89 (m, 2H), 1.88–1.61 (m, 1H), 1.60–1.35 (m, 2H), 0.99–0.97 (m, 6H). ^{13}C NMR (400 MHz, CD_3OD): δ 192.9, 181.5, 173.2, 165.3, 154.7, 138.4, 132.3, 128.5, 127.2, 126.5, 124.3, 123.7, 116.8, 113.1, 69.2, 56.0, 54.2, 42.0, 40.0, 39.8, 34.0, 32.6, 29.2, 28.8, 25.7, 23.4, 22.0, 21.7. HRMS (ESI): *m/z* calcd for $C_{28}H_{32}N_4O_6SNa$ $[M + Na]^+$ 575.1940 found 575.1926.

*4.6.11. (S)-N-((S)-1-(Benzo[d]thiazol-2-yl)-1-oxo-3-((S)-2-oxopyrrolidin-3-yl)propan-2-yl)-2-(2-(3-(dimethylamino)phenoxy)acetamido)-4-methylpentanamide (**26k**)*

Yield 35% from **24a**; light green solid; ^{1}H NMR (400 MHz, $CDCl_3$): δ 8.18 (d, J = 7.6 Hz, 1H), 7.99–7.97 (d, J = 8.0 Hz, 1H), 7.60–7.52 (m, 2H), 7.29–7.22 (m, 1H, merged with $CDCl_3$), 7.11 (d, J = 8.4 Hz, 1H), 6.77–6.70 (m, 1H), 6.56 (dd, 8.1, 8.4 Hz, 2H), 5.70–5.66 (m, 1H), 4.79–4.67 (m, 1H), 4.66–4.50 (m, 2H), 3.41–3.28 (m, 2H), 3.04 (s, 3H), 3.01 (s, 3H), 2.75–2.60 (m, 1H), 2.59–2.49 (m, 1H), 2.48–2.35 (m, 1H), 2.34–2.10 (m, 2H), 2.05–1.85 (m, 1H), 1.79–1.57 (m, 2H), 0.99–0.90 (m, 6H). ^{13}C NMR (400 MHz, CD_3OD): δ 193.6, 181.9, 178.0, 172.3, 171.6, 171.3, 165.7, 142.6, 138.4, 131.2, 129.3, 128.5, 126.8, 123.7, 121.9, 90.7, 77.2, 66.7, 57.4, 52.8, 41.5, 40.0, 33.7, 28.8, 25.7, 23.4, 22.0, 21.7. HRMS (ESI): m/z calcd for $C_{30}H_{38}N_5O_5S$ $[M + H]^+$ 580.2594 found 580.2563.

*4.6.12. (S)-N-((S)-1-(Benzo[d]thiazol-2-yl)-1-oxo-3-((S)-2-oxopyrrolidin-3-yl)propan-2-yl)-2-(2-((4-methoxyphenyl)amino)acetamido)-4-methylpentanamide (**26l**)*

Yield 45% from **24a**; light yellow solid; ^{1}H NMR (400 MHz, CD_3OD): δ 8.24 (d, J = 8.0 Hz, 1H), 8.14 (d, J = 8.0 Hz, 1H), 7.68–7.60 (m, 2H), 7.06 (t, J = 8.4 Hz, 1H), 6.30–6.17 (m, 3H), 5.72–5.68 (m, 1H), 4.53–4.50 (m, 1H), 3.84–3.65 (m, 2H), 3.82 (s, 3H), 3.37–3.28 (m, 2H, merged with CD_3OD), 2.72–2.55 (m, 1H), 2.54–2.29 (m, 1H), 2.28–1.83 (m, 3H), 1.62–1.41 (m, 3H), 0.90–0.83 (m, 6H). ^{13}C NMR (400 MHz, CD_3OD): δ 193.4, 181.8, 175.4, 165.6, 164.0, 155.8, 154.7, 138.3, 132.0, 129.3, 129.2, 128.4, 127.1, 126.4, 124.2, 122.9, 116.7, 113.9, 105.2, 103.2, 56.2, 53.4, 41.8, 40.0, 39.4, 33.9, 29.3, 28.8, 26.1, 22.1, 21.9. HRMS (ESI): m/z calcd for $C_{29}H_{36}N_5O_5S$ $[M + H]^+$ 566.2437 found 566.2428.

*4.6.13. (S)-N-((S)-1-(Benzo[d]thiazol-2-yl)-1-oxo-3-((S)-2-oxopyrrolidin-3-yl)propan-2-yl)-2-(2-((3-methoxyphenyl)amino)acetamido)-4-methylpentanamide (**26m**)*

Yield 41% from **24a**; light yellow solid; ^{1}H NMR (400 MHz, CD_3OD): δ 8.21 (d, J = 7.6 Hz, 1H), 8.12 (d, J = 7.6 Hz, 1H), 7.66–7.58 (m, 2H), 7.10–6.89 (m, 4H), 5.80–5.65 (m, 1H), 4.60–4.45 (m, 1H), 3.94–3.72 (m, 2H), 3.76 (s, 3H), 3.36–3.29 (m, 2H, merged with CD_3OD), 2.75–2.55 (m, 1H), 2.49–2.25 (m, 1H), 2.20–1.80 (m, 3H), 1.70–1.45 (m, 3H), 0.99–0.84 (m, 6H). ^{13}C NMR (400 MHz, CD_3OD): δ 193.4, 181.8, 177.4, 162.3, 160.2, 157.8, 141.2, 138.4, 133.9, 129.3, 128.4, 126.5, 123.7, 119.3, 116.4, 109.9, 66.0, 55.6, 55.4, 53.0, 42.0, 41.7, 41.5, 34.3, 28.8, 25.7, 23.3, 21.9, 21.5. HRMS (ESI): m/z calcd for $C_{29}H_{36}N_5O_5S$ $[M + H]^+$ 566.2437 found 566.2415.

*4.6.14. (S)-N-((S)-1-(Benzo[d]thiazol-2-yl)-1-oxo-3-((S)-2-oxopyrrolidin-3-yl)propan-2-yl)-2-(2-((2-methoxyphenyl)amino)acetamido)-4-methylpentanamide (**26n**)*

Yield 45% from **24a**; light yellow solid; ^{1}H NMR (400 MHz, CD_3OD): δ 8.11 (d, J = 7.6 Hz, 1H), 8.02 (d, J = 7.6 Hz, 1H), 7.56–7.48 (m, 2H), 6.85–6.82 (m, 1H), 6.79–6.87 (m, 2H), 6.56–6.54 (m, 1H), 5.65–5.56 (m, 1H), 4.43–4.39 (m, 1H), 3.81–3.73 (m, 5H), 3.31–3.25 (m, 2H, merged with CD_3OD), 2.58–2.45 (m, 2H), 2.44–2.10 (m, 1H), 2.09–1.68 (m, 3H), 1.40–1.38 (m, 3H), 0.80–0.71 (m, 6H). ^{13}C NMR (400 MHz, CD_3OD): δ 193.4, 181.8, 174.9, 173.3, 165.5, 159.8, 154.4, 138.4, 133.3, 130.2, 129.3, 128.0, 126.9, 123.7, 123.2, 116.3, 65.4, 56.1, 55.4, 53.0, 42.0, 41.6, 40.1, 34.3, 33.7, 28.8, 25.7, 23.3, 21.9, 21.2. HRMS (ESI): m/z calcd for $C_{29}H_{36}N_5O_5S$ $[M + H]^+$ 566.2437 found 566.2426.

4.7. Synthesis of **27**

Compounds **27a**–**d** were prepared from **24b**–**d** with **20a** using a similar procedure to that described for the synthesis of **25a**.

*4.7.1. Benzyl ((S)-4-methyl-1-oxo-1-(((S)-1-oxo-3-((S)-2-oxopyrrolidin-3-yl)-1-(5-phenylthiazol-2-yl)propan-2-yl)amino)pentan-2-yl)carbamate (**27a**)*

Yield 55% from **24b**; colorless solid; ^{1}H NMR (400 MHz, CD_3OD): δ 8.32–8.30 (m, 1H), 7.72 (d, J = 7.20 Hz, 2H), 7.48–7.40 (m, 3H), 7.37–7.24 (m, 5H), 5.65–5.61 (m, 1H), 5.15–5.03 (m, 2H), 4.30–4.20 (m, 1H), 3.40–3.23 (m, 2H, merged with CD_3OD), 2.75–2.65 (m, 1H), 2.64–2.06 (m, 2H), 2.05–1.80 (m, 2H), 1.79–1.60 (m, 1H), 1.59–1.52 (m, 2H), 0.99–0.89 (m, 6H). ^{13}C NMR (400 MHz, CD_3OD): δ 192.0, 181.8, 175.8, 164.2, 158.4, 148.9, 141.9, 131.5, 130.9, 130.7, 129.4, 128.9, 128.7, 128.3, 67.7, 61.5, 55.7, 54.8, 42.4, 41.5, 40.1, 38.9, 34.2, 29.3, 28.6, 25.9, 24.2, 23.4, 22.1, 21.8. HRMS (ESI): m/z calcd for $C_{30}H_{35}N_4O_5S$ $[M + H]^+$ 563.2328 found 563.2308.

*4.7.2. Benzyl ((S)-4-methyl-1-oxo-1-(((S)-1-oxo-3-((S)-2-oxopyrrolidin-3-yl)-1-(5-(p-tolyl)thiazol-2-yl)propan-2-yl)amino)pentan-2-yl)carbamate (**27b**)*

Yield 51% from **24c**; colorless solid; ^{1}H NMR (400 MHz, CD_3OD): δ 8.32–8.29 (m, 1H), 7.62 (d, J = 8.4 Hz, 2H), 7.40–7.20 (m, 7H), 5.70–5.57 (m, 1H), 5.15–5.01 (m, 2H), 4.30–4.18 (m, 1H), 3.40–3.25 (m, 2H, merged with CD_3OD), 2.75–2.40 (m, 1H), 2.50–2.30 (m, 2H), 2.38 (s, 3H), 2.29–2.09 (m, 1H), 2.08–1.75 (m, 2H), 1.74–1.65 (m, 1H), 1.63–1.49 (m, 2H), 0.97–0.90 (m, 6H). HRMS (ESI): m/z calcd for $C_{31}H_{37}N_4O_5S$ $[M + H]^+$ 577.2485 found 577.2484.

*4.7.3. Benzyl ((S)-1-(((S)-1-(5-(4-methoxyphenyl)thiazol-2-yl)-1-oxo-3-((S)-2-oxopyrrolidin-3-yl)propan-2-yl)amino)-4-methyl-1-oxopentan-2-yl)carbamate (**27c**)*

Yield 47% from **24d**; light yellow solid; ^{1}H NMR (400 MHz, $CDCl_3$): δ 8.05–8.03 (m, 1H), 7.60–7.52 (m, 2H), 7.60–7.27 (m, 5H), 7.00–6.95 (m, 2H), 5.64–5.56 (m, 1H), 5.20–5.08 (m, 1H), 4.40–4.25 (m, 1H), 3.86 (s, 3H), 3.35–3.34 (m, 2H), 2.67–2.42 (m, 2H), 2.22–2.04 (m, 2H), 2.02–1.96 (m, 1H), 1.80–1.52 (m, 3H), 0.97–0.86 (m, 6H). HRMS (ESI): m/z calcd for $C_{31}H_{37}N_4O_6S$ $[M + H]^+$ 593.2434 found 593.2414.

*4.7.4. Benzyl ((S)-1-(((S)-1-(5-(2-methoxyphenyl)thiazol-2-yl)-1-oxo-3-((S)-2-oxopyrrolidin-3-yl)propan-2-yl)amino)-4-methyl-1-oxopentan-2-yl)carbamate (**27d**)*

Yield 51% from **24e**; light yellow solid; ^{1}H NMR (400 MHz, $CDCl_3$): δ 8.12–8.10 (m, 1H), 7.37–7.27 (m, 6H), 7.19 (d, J = 7.6 Hz, 1H), 7.13–7.11 (m, 1H), 6.95 (dd, 1.8, 8.2 Hz, 1H), 5.70–5.53 (m, 1H), 5.15–5.08 (m, 2H), 4.40–4.30 (m, 1H), 3.85 (s, 3H), 3.50–3.25 (m, 2H), 2.70–2.37 (m, 2H), 2.35–2.05 (m, 2H), 2.04–1.80 (m, 1H), 1.79–1.60 (m, 2H), 1.59–1.45 (m, 1H), 0.99–0.80 (m, 6H). ^{13}C NMR (400 MHz, $CDCl_3$): δ 190.8, 180.3, 172.8, 162.9, 160.1, 156.1, 147.4, 140.6, 136.4, 131.5, 130.4, 128.4, 127.9, 119.7, 115.1, 113.1, 66.8, 55.4, 53.4, 42.2, 41.7, 40.7, 38.9, 33.5, 31.9, 28.2, 24.7, 24.6, 23.0, 22.9, 22.0. HRMS (ESI): m/z calcd for $C_{31}H_{37}N_4O_6S$ $[M + H]^+$ 593.2434 found 593.2427.

4.8. Molecular docking studies

The crystal structure of the SARS-CoV 3CL protease in complex with a substrate analog inhibitor (coded 1WOF) [35] was obtained from the Protein Data Bank (PDB; http://www.rcsb.org/pdb/home/home.do). Initially, a binding model of **26m** with $3CL^{pro}$ was simulated to form the basis of a comparison with our previous potent lead tripeptidomimetic **9** and a substrate analog, using molecular operating environment (MOE) software. Several minimization processes were performed using the MMFF94X force field to model the solvation environment surrounding the inhibitor. Structures having a relatively low binding free energy and a high number of cluster members were selected for the subsequent docking conformation optimization step. The minimized energies

of **26m**, obtained from the docking study, were −40.67 and −35.52 kcal/mol.

Acknowledgments

This research was supported by Grants from the Ministry of Education, Culture, Sports, Science and Technology (MEXT) of Japan, including a Grant-in-aid for Young scientist (Tokubetsu Kenkyuin Shorei-hi) 23·01104 and a Grant-in-aid for Scientific Research 23659059 and 23390029. E.F. acknowledges support from the National Institutes of Health (grant GM57144).

Appendix A. Supplementary data

Supplementary data related to this article can be found at http://dx.doi.org/10.1016/j.ejmech.2013.05.005.

References

[1] C. Drosten, S. Gunther, W. Preiser, S. Ven der Werf, H.R. Brodt, S. Becker, H. Rabenau, M. Panning, L. Kolensnikova, R.A.M. Fouchier, A. Berger, A.M. Burguiere, J. Cinatl, M. Eickmann, N. Escriou, K. Grywna, S. Kramme, J. Manuguerra, S. Muller, V. Rickerts, M. Sturmer, S. Vieth, H.D. Klenk, A.D.M.E. Osterhaus, H. Schmitz, H.W. Doerr, N. Engl. J. Med. 348 (2003) 1967–1976.
[2] N. Lee, D. Hui, A. Wu, P. Chan, P. Cameron, F.M. Joynt, A. Ahuja, M.Y. Yung, C.B. Leung, K.F. To, M.D. Leu, C.C. Szeto, S. Chung, J.J.Y. Sung, N. Engl. J. Med. 348 (2003) 1986–1994.
[3] T.G. Ksiazek, D. Erdman, C.S. Goldsmith, S.R. Zaki, T. Peret, S. Emery, S. Tong, C. Urbani, J.A. Comer, W. Lim, P.E. Rollin, S.F. Dowell, A.E. Ling, C.D. Humphrey, W.J. Shieh, J. Guarner, C.D. Paddock, P. Rota, B. Fields, J. DeRisi, J.Y. Yang, N. Cox, J.M. Hughes, J.W. LeDuc, W.J. Bellini, L.J. Anderson, N. Engl. J. Med. 348 (2003) 1953–1966.
[4] K. Anand, J. Ziebuhr, P. Wadhwani, J.R. Mesturs, R. Hilgenfeld, Science 300 (2003) 1763–1767.
[5] J.S. Peiris, S.T. Lai, L.L. Poon, Y. Guan, L.Y. Yam, W. Lim, J. Nicholls, W.K. Yee, W.W. Yan, M.T. Cheung, V.C. Cheng, K.H. Chan, D.N. Tsang, R.W. Yung, T.K. Ng, K.Y. Yuen, Lancet 361 (2003) 1319–1325 (and references therein).
[6] P.A. Rota, M.S. Oberste, S.S. Monroe, W.A. Nix, R. Campagnoli, J.P. Icenogle, S. Penaranda, B. Bankamp, K. Maher, M.H. Chem, W. Tong, A. Tamin, L. Lowe, M. Frace, J.L. DeRisi, Q. Chen, D. Wang, D.D. Erdman, T.C. Peret, C. Burns, T.G. Ksiazek, P.E. Rollin, A. Sanchez, S. Liffick, B. Holloway, J. Limor, K. McCaustland, M. Olsen-Rasmussen, R. Fouchier, S. Gunther, A.D. Osterhaus, C. Drosten, M.A. Pallansch, L.J. Anderson, W.J. Bellini, Science 300 (2003) 1394–1399.
[7] M.A. Marra, S.J. Jones, C.R. Astell, R.A. Holt, A. Brooks-Wilson, Y.S. Butterfield, J. Khattra, J.K. Asano, S.A. Barber, S.Y. Chan, A. Cloutier, S.M. Coughlin, D. Freeman, N. Girn, O.L. Griffith, S.R. Leach, M. Mayo, H. McDonald, S.B. Montgomery, P.K. Pandoh, A.S. Petrescu, A.G. Robertson, J.E. Schein, A. Siddiqui, D.E. Smailus, J.M. Sott, G.S. Yang, F. Plummer, A. Andonov, H. Artsob, N. Bastien, K. Bermard, T.F. Booth, D. Bowness, M. Czub, M. Drebot, L. Fernando, R. Flick, M. Garbutt, M. Gray, A. Grolla, S. Jones, H. Feldmann, A. Meyers, A. Kabani, Y. Li, S. Normand, U. Stroher, G.A. Tipples, S. Tyler, R. Vogrig, D. Ward, B. Watson, R.C. Brunham, M. Krajden, M. Petric, D.M. Skowronski, C. Upton, R.L. Roper, Science 300 (2003) 1399–1404.
[8] V. Thiel, K.A. Ivanov, A.A. Putics, T. Hertzig, B. Schelle, S. Bayer, B. Weiabrich, E.J. Snijder, H. Rabenau, H.W. Doerr, J. Ziebuhr, J. Gen. Virol. 84 (2003) 2305–2315.
[9] H. Yang, M. Yang, Y. Ding, Y. Liu, Z. Lou, Z. Zhou, L. Sun, L. Mo, S. Ye, H. Pang, G.F. Gao, K. Anand, M. Bartlam, R. Hilgenfeld, Z. Rao, Proc. Natl. Acad. Sci. U. S. A. 100 (2003) 13190–13195.
[10] K. Chou, D. Wei, W. Zhong, Biochem. Biophys. Res. Commun. 308 (2003) 148–151.
[11] K. Pyrc, B. Berkhout, L. van der Hoek, J. Virol. 81 (2007) 3051–3057.
[12] B.C. Fielding, Future Microbiol. 6 (2011) 153–159.
[13] A.M. Zaki, S. van Boheemen, T.M. Bestebroer, A.D.M.E. Osterhaus, R.A.M. Fouchier, N. Engl. J. Med. 367 (2012) 1814–1820.
[14] http://www.independent.co.uk/life-style/health-and-families/health-news/sarslike-virus-spreads-persontoperson-in-the-uk-8492750.html.
[15] Y.M. Shao, W.B. Yang, T.H. Kuo, K.C. Tsai, C.H. Lin, A.S. Yang, P.H. Liang, C.H. Wong, Bioorg. Med. Chem. 16 (2008) 4652–4660.
[16] R.P. Jain, H.I. Pettersson, J. Zhang, K.D. Aull, P.D. Fortin, C. Huitema, L.D. Eltis, J.C. Parrish, M.N. James, D.S. Wishart, J.C. Vederas, J. Med. Chem. 47 (2004) 6113–6116.
[17] S. Yang, S.J. Chen, M.F. Hsu, J.D. Wu, C.T. Tseng, Y.F. Liu, H.C. Chen, C.W. Kuo, C.S. Wu, L.W. Chang, W.C. Chen, S.Y. Liao, T.Y. Chang, H.H. Hung, H.L. Shr, C.Y. Liu, Y.A. Huang, L.Y. Chang, J.C. Hsu, C.J. Peters, A.H. Wang, M.C. Hsu, J. Med. Chem. 49 (2006) 4971–4980.
[18] T.W. Lee, M.M. Cherney, C. Huitema, J. Liu, K.E. James, J.C. Powers, L.D. Eltis, M.N.G. James, J. Mol. Biol. 353 (2005) 1137–1151.
[19] K. Akaji, H. Konno, H. Mitsui, K. Teruya, Y. Shimamoto, Y. Hattori, T. Ozaki, M. Kusunoki, A. Sanjoh, J. Med. Chem. 54 (2011) 7962–7973.
[20] M.O. Sydnes, Y. Hayashi, V.K. Sharma, T. Hamada, U. Bacha, J. Barrila, E. Freire, Y. Kiso, Tetrahedron 62 (2006) 8601–8609.
[21] T. Regnier, D. Sharma, K. Hidaka, U. Bacha, E. Freire, Y. Hayashi, Y. Kiso, Bioorg. Med. Chem. Lett. 19 (2009) 2722–2727.
[22] S. Konno, P. Thanigaimalai, K. Nakada, T. Yamamoto, Y. Yamazaki, F. Yakushiji, K. Akaji, Y. Kiso, Y. Kawasaki, E. Freire, Y. Hayashi, Bioorg. Med. Chem. 21 (2013) 412–424.
[23] U. Kaeppler, N. Stiefl, M. Schiller, R. Vicik, A. Breuning, W. Schmitz, D. Rupprecht, C. Schmuck, K. Baumann, J. Ziebuhr, T. Schirmeister, J. Med. Chem. 48 (2005) 6832–6842.
[24] L. Chen, C. Gui, X. Luo, Q. Yang, S. Gunther, E. Scandella, C. Drosten, D. Bai, X. He, B. Ludewig, J. Chen, H. Luo, Y. Yang, Y. Yang, J. Zou, V. Thiel, K. Chen, J. Shen, X. Shen, H. Jiang, J. Virol. 79 (2005) 7095–7103.
[25] J.E. Blanchard, N.H. Elowe, C. Huitema, P.D. Fortin, J.D. Cechetto, L.D. Eltis, E.D. Brown, Chem. Biol. 11 (2004) 1445–1453.
[26] L. Zhou, Y. Liu, W. Zhang, P. Wei, C. Huang, J. Pei, Y. Yuan, L. Lai, J. Med. Chem. 49 (2006) 3440–3443.
[27] C.Y. Wu, K.Y. King, C.J. Kuo, J.M. Fang, Y.T. Wu, M.Y. Ho, C.L. Liao, J.J. Shie, P.H. Liang, C.H. Wong, Chem. Biol. 13 (2006) 261–268.
[28] R. Ramajayam, K.P. Tan, H.G. Liu, P.H. Liang, Bioorg. Med. Chem. Lett. 20 (2010) 3569–3572.
[29] R. Ramajayam, K.P. Tan, H.G. Liu, P.H. Liang, Bioorg. Med. Chem. 18 (2010) 7849–7854.
[30] P. Mukherjee, P. Desai, L. Ross, E.L. White, M.A. Avery, Bioorg. Med. Chem. 7 (2008) 4138–4149.
[31] Q. Tian, N.K. Nayyar, S. Babu, L. Chen, J. Tao, S. Lee, A. Tibbetts, T. Moran, J. Liou, M. Guo, T.P. Kennedy, Tetrahedron Lett. 42 (2001) 6807–6809.
[32] U. Bacha, J. Barrila, B. Gabelli, Y. Kiso, L.M. Amzel, E. Freire, Chem. Biol. Drug Des. 72 (2008) 34–39.
[33] J. Barrila, U. Bacha, E. Freire, Biochemistry 45 (2006) 14908–14916.
[34] K. Akaji, H. Konno, M. Onozuka, A. Makino, H. Saito, K. Nosaka, Bioorg. Med. Chem. 16 (2008) 9400–9408.
[35] H. Yang, W. Xie, X. Xue, K. Yang, J. Ma, W. Liang, Q. Zhao, Z. Zhou, D. Pei, J. Ziebuhr, R. Hilgenfeld, K.Y. Yuen, L. Wong, G. Gao, S. Chen, Z. Chen, D. Ma, M. Bartlam, Z. Rao, PLoS Biol. 3 (2005) 1742–1752.